MICHIGAN STATE UNIVERSITY

CYCLOTRON LABORATORY

CANONICAL ENSEMBLES FROM CHAOS
I: CLASSICAL SYSTEMS

D. KUSNEZOV, A. BULGAC and W. BAUER

JANUARY 1990

MSUCL-711

CANONICAL ENSEMBLES FROM CHAOS
I: CLASSICAL SYSTEMS

DIMITRI KUSNEZOV, AUREL BULGAC AND WOLFGANG BAUER

National Superconducting Cyclotron Laboratory
and Department of Physics *and Astronomy,*
Michigan *State* University, *East* Lansing, MI *48824-1321*

ABSTRACT

We present methods to compute thermodynamic properties of classical sys-*tems which* involve *extending the phase space by two degrees of freedom. These two additional degrees of freedom are used to replicate the coupling of the* orig-*inal system to the* infinite *degrees of freedom of a heat bath. In* the extended *phase space, the trajectories are ergodic. This feature enables one to* replace *phase space averages by time averages, which are extremely simple to compute. We examine phase space patterns, thermal distributions,* correlations, *ergodicity, Lyapunov exponents, mixing and rate of convergence in au analysis of several simple systems.*

PACS numbers: 05.20.Gg, 05.20.-y, 82.20.Fd

1. INTRODUCTION

One is often encountered with the need to evaluate finite temperature expectation values of operators for many body systems. Generally one can resort to Monte-Carlo simulations, but in some cases such methods are inadequate. In lattice gauge theories the handling of dynamical fermions provides such an example. Alternate schemes include the introduction of Langevin terms, however this has the disadvantage of requiring many iterations to achieve thermalization. In dealing with stochastic systems for which the ergodic theorems hold, canonical averages are simply evaluated from the time averaged operators over the trajectories. However, in most cases we do not have an *a priori* ergodic dynamics. The methods we study here begin with an arbitrary $2N$ dimensional classical Hamiltonian system H, which can be regular and even completely integrable. The phase space is extended to $2N+2$ dimensions, in which the classical trajectories become ergodic. The two additional degrees of freedom are introduced in such a way that they replicate the coupling of the original system H to the infinite degrees of freedom of a heat bath at temperature T. All the properties of the original system H will then be seen to be preserved on average in the extended phase space. The central question of ergodicity has only been addressed tangentially in the past. The usual assumption is that the many body problem is sufficiently complex that ergodicity is guaranteed. However, we demonstrate that the models used previously do not lead to ergodic dynamics in the extended phase space in simple solvable systems, whereas the present generalized couplings do produce ergodicity while retaining at the same time simplicity.

Numerical simulations of non-equilibrium systems have been intensely studied for many years [1] . But it was only a decade ago that molecular dynamics (MD) methods were introduced to model a system interacting with a constant temperature heat bath [2] . Two years later, Hoover *et al* introduced a non-equilibrium MD constant temperature method in which pseudo-friction terms were added to equations of motion [3] . These terms are referred to as pseudo-frictions since they appear in the equations of motion in the form of velocity dependent forces. These results were made more precise several years ago when Nosé demonstrated that the coupling of a 2N dimensional classical system to a constant temperature heat bath can be emulated by simply adding a single degree of freedom to the original system [4] . It was shown that in this case the canonical ensemble of the original system is equivalent to the microcanonical ensemble of the extended system. However, Nosé's method relied on the assumption that the dynamics is ergodic, which does not necessarily follow from the formulation of the problem. Nosé's equations of motion were later recast by Hoover [5] to demonstrate the equivalent interpretation in terms of the addition of a velocity dependent force

to the equations of motion. The principle behind these methods is that in this extended 2N+1 dimensional phase space, the trajectories are deterministic and can also be chaotic for suitable choices of parameters. In the chaotic regime, canonical ensemble averages are equivalent to time averages over the trajectories, which can be computed easily by simply following the time evolution of the system for some time.

One of the principal difficulties with the Nosé-Hoover formulations is the unpredictability of non-ergodicity. Indeed, the solvable models that have been studied in the past have been chaotic at best, but not ergodic. There is strong dependence on initial conditions, parameters and forms of the pseudo-friction term. As we have stated, Nosé's method [4] is no longer valid if the chaotic trajectories are only recurrent and not ergodic. When non-ergodic chaos occurs or the system is only intermittently chaotic, only limited regions of the phase space are reached, and there is no way to reproduce the canonical ensemble. There are additional peculiarities. For example, even if a system is chaotic at some temperature T, it is not necessarily chaotic at other temperatures. A particular problem lies in the description of systems with harmonic oscillator potentials at any T. For low T, this leads to difficulties, as the system will remain close to the minimum of the potential, which in many cases is harmonic in character. Further, there has been no general understanding of when such methods produce truly ergodic dynamics. As we demonstrate below, this limitation is a manifestation of the form of the coupling of the system to the heat bath. A suitable generalization of this coupling can produce ergodic behavior, reproducing the canonical ensemble averages.

A better understanding is clearly required in order to develop methods for systems with curved phase spaces (such as Lie algebras) where the Nosé method is not applicable as well as quantum systems. Examples of such systems are constrained dynamical systems. In a recent letter we proposed methods to extend the Nosé-Hoover dynamics to classical Lie algebras as well as to quantum systems [6] . The ambition of our program is to provide a reliable well defined procedure that can rival Monte-Carlo methods, in which finite temperature expectation values can be rapidly constructed via deterministic ergodic time evolution. With respect to practical applications, it is of particular importance that these methods converge to the correct results independent of initial conditions chosen. This work is the first of several detailed articles on this subject. In following papers we examine the extension of these methods to constrained dynamical systems, in particular those Hamiltonians which can be written in terms of generators of Lie algebras [7] . Additionally, we will discuss extensions to quantum mechanical systems. The outline of this paper is as follows. In Section 2, we introduce our extended dynamics. In Section 3 we detail explicitly the results for 1 and

2 dimensional systems. This includes discussion of the properties of a coupling scheme that results in ergodic dynamics. We conclude in section 4.

2. THEORETICAL CONSIDERATIONS

It is instructive to briefly review Nosé's dynamics [4] . We begin with a Hamiltonian H and a 2N dimensional phase space $(q_1, ..., q_N, p_1, ..., p_N)$ governed by the usual Hamilton equations of motion

$$\begin{aligned} H &= \sum_{i=1}^{N} \frac{p_i^2}{2m_i} + V(q), \\ \frac{dq_i}{dt} &= \frac{\partial H}{\partial p_i}, \\ \frac{dp_i}{dt} &= -\frac{\partial H}{\partial q_i}. \end{aligned} \tag{1}$$

In Nosé's scenario, the fixed temperature canonical ensemble can be simulated by the addition of a single variable s. In this extended phase space, the external system (heat bath) is assumed to interact in such a way as to scale the velocities $v_i = s\dot{q}_i$. Nosé interpreted the scaled velocity v_i as the true velocity resulting from heat exchange with the external system. An augmented Lagrangian is introduced in the form

$$\mathcal{L} = \sum_{i=1}^{N} \frac{m_i}{2} s^2 \dot{q}_i^2 - V(q) + \frac{1}{2\alpha}\dot{s}^2 - (N+1)T \ln s. \tag{2}$$

Here N is the number of degrees of freedom of the system and T is the temperature. The logarithmic character of the "potential energy" of the heat bath is introduced to achieve the equivalence of the canonical ensemble for the original system (1) with the microcanonical ensemble for the augmented system. The momenta in this extended space are

$$p_i = \frac{\partial \mathcal{L}}{\partial \dot{q}_i} = m_i s^2 \dot{q}_i, \qquad p_s = \frac{\partial \mathcal{L}}{\partial \dot{s}} = \frac{\dot{s}}{\alpha}. \tag{3}$$

The corresponding Hamiltonian and the equations of motion are easily obtained

$$H' = \sum_{i=1}^{N} \frac{p_i^2}{2m_i s^2} + V(q) + \alpha\frac{p_s^2}{2} + (N+1)T \ln s, \tag{4}$$

$$
\begin{aligned}
\dot{q}_i &= \frac{p_i}{m_i s^2}, \\
\dot{p}_i &= -\frac{\partial V}{\partial q_i}, \\
\dot{s} &= \alpha p_s, \\
\dot{p}_s &= \frac{1}{s}\left(\sum_{i=1}^{N} \frac{p_i^2}{m_i s^2} - (N+1)T\right).
\end{aligned}
\tag{5}
$$

For any solution to (5), H' is conserved exactly. What Nosé demonstrated is that in this extended phase space, the microcanonical ensemble of H' is precisely the canonical ensemble of H at temperature T. To prove this, the microcanonical ensemble partition function is defined by

$$
Z = \int dp_s ds \prod_i dp_i dq_i \; \delta(H' - E). \tag{6}
$$

By rescaling $P_i = p_i/s$ we obtain

$$
Z = \int dp_s ds \; s^N \prod_i dP_i dq_i \delta(H + \frac{\alpha}{2} p_s^2 + (N+1)T \ln s - E). \tag{7}
$$

The H that appears in (7) is the original Hamiltonian of (1). The integral over s is easily completed using the delta function property $\delta(f(s)) = \delta(s - s_0)/|f'(s_0)|$, where $f(s_0) = 0$ and $f'(s_0) \neq 0$:

$$
\begin{aligned}
&\int ds \; s^N \delta(H + \frac{\alpha}{2} p_s^2 + (N+1)T \ln s - E) \\
&\qquad = \int ds \; s^N \frac{s}{(N+1)T} \delta\left(s - e^{-(H + \frac{\alpha}{2} p_s^2 - E)/((N+1)T)}\right) \\
&\qquad = \frac{1}{(N+1)T} e^{-[H + \frac{\alpha}{2} p_s^2 - E]/T}.
\end{aligned}
\tag{8}
$$

The resulting partition function can be expressed as

$$
Z = const \int \prod_i dP_i dq_i e^{-H/T}. \tag{9}
$$

The constant term represents the p_s gaussian integration and the remaining constants. This expression is the partition function for the canonical ensemble for the initial Hamiltonian H.

The next step is to impose the quasi-ergodic hypothesis. This asserts that the time average is equivalent to the microcanonical ensemble average in the extended phase space, and hence to the canonical ensemble in the original phase space. If the equations of motion for H' do not lead to truly ergodic motion, this is clearly incorrect. If it does lead to ergodic motion, the results follow trivially from classical ergodic theory since the measure on the extended phase space has the density $\exp(-H'/T)$. In summary, Nosé's dynamics consists of augmenting an arbitrary Hamiltonian H to produce the extended phase space Hamiltonian H'. The essential idea is that the infinite dimensional heat bath can be mocked by a single degree of freedom s. If the Hamiltonian is ergodic, time averages in the extended system correspond to canonical ensemble averages in the original system.

In Nosé's formulation, a 'true' time step dt' can be defined by $\dot{v}_i = dq_i/dt'$, where the true (scaled) time interval is $dt' = dt/s$. Since s is a dynamic variable, the time intervals dt' evolve dynamically in time. An equivalent formulation of the Nosé equations of motion in terms of scaled time is

$$\begin{aligned}
\frac{\partial q_i}{\partial t'} &= \frac{p_i}{m_i s}, \\
\frac{\partial p_i}{\partial t'} &= -s\frac{\partial V}{\partial q_i}, \\
\frac{\partial s}{\partial t'} &= s\alpha p_s, \\
\frac{\partial p_s}{\partial t'} &= \sum_i \frac{p_i^2}{m_i s^2} - (N+1)T.
\end{aligned} \tag{10}$$

In Hoover's reformulation of the Nosé equations of motion (5), the variable s is removed, and the equations of motion for s and $\dot{s}$ are replaced by a single equation. The resulting set of equations is much simpler to analyze. We begin by defining the new thermodynamic pseudo-friction coefficient

$$\zeta = \frac{1}{s}\frac{ds}{dt'} = \alpha p_s. \tag{11}$$

Then by defining $q_i' = q_i$ and $p_i' = m_i dq_i/dt' = p_i/s$, and replacing Nosé's (N+1) factor by N, we arrive at Hoover's equations of motion, which we hereafter refer to as the Nosé-Hoover equations [5] . It is convenient at this point to drop the primes in the notation for the variables q_i, p_i, ζ and t. The Nosé-Hoover equations

of motion are:

$$\begin{aligned} \dot{q}_i &= p_i/m_i, \\ \dot{p}_i &= -\frac{\partial V}{\partial q_i} - \zeta p_i, \\ \dot{\zeta} &= \alpha \left(\sum_{i=1}^{N} \frac{p_i^2}{2m_i} - NT \right). \end{aligned} \tag{12}$$

These equations of motion no longer retain a Hamiltonian structure. In the extended phase space the variables q_i, p_i and ζ are no longer canonical and the symplectic structure is lost. One manifestation of this formulation is that the pseudo-Hamiltonian of the extended system (q_i, p_i, ζ) assumes a more complicated form. This quantity is referred to as the pseudo-energy. In terms of (q_i, p_i, ζ), the Nosé Hamiltonian is replaced by a pseudo-energy of this system

$$\mathcal{E} = \sum_{i=1}^{N} \frac{p_i^2}{2m_i} + V(q) + \frac{\zeta^2}{2\alpha} + T \int_0^t \zeta(t')dt', \tag{13}$$

where $\dot{\mathcal{E}} = 0$ is easily verified by direct substitution of the equations of motion. Finally, on average one has

$$\left\langle \frac{1}{N} \sum_{i=1}^{N} p_i^2 \right\rangle = \left\langle \frac{1}{N} \sum_{i=1}^{N} q_i \frac{\partial V}{\partial q_i} \right\rangle = \left\langle \frac{\zeta^2}{\alpha} \right\rangle = T. \tag{14}$$

2.1 Ergodic and Non-Ergodic Motion

The tremendous literature on chaos in the past ten years has, among other things, produced a classification of different types of chaotic behavior. For the reader unfamiliar with some of this terminology, we present relevant definitions that will be used below. To begin with, for an arbitrary function $A(q,p)$, we define the phase space average $\langle A(q,p) \rangle$ and the time average $\overline{A}(q,p)$ as

$$\langle A(q,p) \rangle = \int d\mu \; A(q,p), \qquad \overline{A}(q,p) = \frac{1}{t} \int_0^t dt' \; A(q(t'), p(t')). \tag{15}$$

Here $d\mu$ is the phase space measure. In this study, our measure will have a Boltzmann factor density $\exp(-H/T)$. A system is then defined to be *ergodic* if

[8]

$$\langle A(q,p)\rangle = \overline{A}(q,p), \tag{16}$$

except on a set of measure zero. If the system is ergodic, these averages are *independent* of the initial conditions. This is an important requirement for convergence of the algorithm for a general Hamiltonian.

It is not necessary for the condition (16) to be satisfied, even for trajectories whose phase-space diagrams are dense. A system is *recurrent* if the trajectories are chaotic but the integral over the phase space measure does not correspond to the time average. This definition usually refers to trajectories that are dense in (possibly disconnected) regions of phase space.

Another often encountered definition is *mixing*. A system is *mixing* if correlations vanish on long (possibly infinite) time scales. A system that is *mixing* is ergodic, but the converse is not always true.

We will use these definitions to distinguish between cases where the thermal distributions are quite different, although the phase space portraits look identical. All these types of motion are referred to as chaotic.

2.2 Equations of Motion

There is no reason we should be limited to the original form of the Nosé-Hoover equations (12). As we shall see in many examples below, their coupling is often not ergodic or even chaotic, whereas suitable generalizations will provide ergodic trajectories. Let us consider a more general formulation, where the Hamilton equations of motion are coupled to a heat bath as follows

$$\begin{aligned} \frac{dq_i}{dt} &= \frac{\partial H}{\partial p_i} - h_1(\xi)F_i(q,p), \\ \frac{dp_i}{dt} &= -\frac{\partial H}{\partial q_i} - h_2(\zeta)G_i(q,p). \end{aligned} \qquad (i = 1,...,N) \tag{17}$$

We restrict ourselves to the case were the arbitrary functions h_1 and h_2 are only functions of ξ and ζ, which turns out to be sufficiently general. By choosing h_1 and h_2 to be functions of both ζ and ξ, the equations of motion for ζ and ξ become more difficult to separate and a self-consistent solution is required (see below). Looking back at the Nosé-Hoover equations ($h_1 \equiv F \equiv 0, h_2 = \zeta, G_i = p_i$), the solution for $q_i(t)$ is (with $m_i = 1$)

$$q_i(t) = q_i(0) + \int_0^t dt'\, p_i(t'). \tag{18}$$

It can be expected in this case that the distributions of momenta can strongly

influence those for coordinates. h_1 and h_2 have been introduced in (17) to better decorrelate q_i and p_i, and ζ and ξ do not correspond to canonical variables.

In the next step we introduce the phase space probability $f(q,p,\zeta,\xi)$ for this 2N+2 dimensional space. Since the variables q_i, p_i, ζ and ξ are independent, we choose the form

$$f(q,p,\zeta,\xi) = \mathcal{N} \exp\Big(-\frac{1}{T}\Big\{ H(q,p) + \frac{1}{\alpha} g_1(\zeta) + \frac{1}{\beta} g_2(\xi) \Big\}\Big). \tag{19}$$

Here $\mathcal{N}$ is a normalization constant, and α and β are at the moment free parameters, although their values are linked to the appearance of chaos. The function f defines the measure on the phase space:

$$\int d\mu\, (\cdots) = \int f \prod_i dp_i dq_i d\zeta d\xi\, (\cdots). \tag{20}$$

In f, the functions g_1 and g_2 that determine the thermal distribution in ζ and ξ are arbitrary. The choice of g_1 and g_2 as pure quadratic (producing gaussian distributions) will often be seen to be inadequate. Since the equations (17) are no longer Hamiltonian, the usual conditions leading to the Liouville equation are no longer valid. That is, for each i

$$\frac{\partial \dot{q}_i}{\partial q_i} + \frac{\partial \dot{p}_i}{\partial p_i} \neq 0, \qquad (i = 1, ..., N). \tag{21}$$

This is easily interpreted as the boundaries of the 2N dimensional (q,p) phase space evolving in time due to the flow in the ζ and ξ directions. This is a consequence of the fact that the augmented phase space is not endowed with a symplectic structure. To obtain conservative time evolution of the probability distribution f, the more general statement of the Liouville equation must be used

$$\frac{\partial f}{\partial t} + \sum_{i=1}^{N} \left[\frac{\partial (f\dot{q}_i)}{\partial q_i} + \frac{\partial (f\dot{p}_i)}{\partial p_i} \right] + \frac{\partial (f\dot{\zeta})}{\partial \zeta} + \frac{\partial (f\dot{\xi})}{\partial \xi} = 0. \tag{22}$$

In order to derive equations of motion for ζ and ξ that reproduce the thermal distribution postulated in (19), we simply substitute the equations of motion (17) and the postulated probability distribution (19) into the Liouville equation (22). This provides a self consistent set of equations in $\dot{\zeta}$ and $\dot{\xi}$. However, by requiring

that

$$\frac{\partial \dot{\zeta}}{\partial \zeta} = 0, \qquad \frac{\partial \dot{\xi}}{\partial \xi} = 0, \tag{23}$$

these equations can be easily solved to obtain

$$\begin{aligned} \dot{\zeta} &= \alpha \left[\frac{h_1}{dg_1/d\zeta} \right] \left(\frac{\partial H}{\partial p_i} G_i - T \frac{\partial G_i}{\partial p_i} \right), \\ \dot{\xi} &= \beta \left[\frac{h_2}{dg_2/d\xi} \right] \left(\frac{\partial H}{\partial q_i} F_i - T \frac{\partial F_i}{\partial q_i} \right). \end{aligned} \tag{24}$$

In order to achieve self-consistency with the requirements (23), the terms in square brackets must be independent of ζ and ξ. This places the restrictions that the thermal distributions $g_1(\zeta)$ and $g_2(\xi)$ introduced in (19) must be integrals of the functions $h_1(\zeta)$ and $h_2(\xi)$ introduced in (17):

$$\begin{aligned} \frac{dg_1}{d\zeta} &= c_1 h_1, \\ \frac{dg_2}{d\xi} &= c_2 h_2, \end{aligned} \tag{25}$$

where c_1 and c_2 are constants. Since these constants can be absorbed into the definitions of α and β in (19), we will always set $c_1 = c_2 = 1$. Thus we have the self-consistent requirements that the thermal distributions and the pseudo-friction terms are related by

$$\begin{aligned} h_1 &\equiv \frac{dg_1}{d\zeta}, \\ h_2 &\equiv \frac{dg_2}{d\xi}. \end{aligned} \tag{26}$$

For this choice it is trivial to check that the thermal averages $\langle h_1 \rangle = \langle h_2 \rangle = 0$, precisely analogous to $\langle \zeta \rangle = 0$ for the gaussian thermal distribution in ζ. When the system is ergodic, this means that the time average also vanishes by (16). The most general equations of motion are henceforth given by

$$\begin{aligned} \dot{q}_i &= \frac{\partial H}{\partial p_i} - h_2 F_i, \\ \dot{p}_i &= -\frac{\partial H}{\partial q_i} - h_1 G_i, \\ \dot{\zeta} &= \alpha \left(\frac{\partial H}{\partial p_i} G_i - T \frac{\partial G_i}{\partial p_i} \right), \qquad (i = 1, ..., N) \\ \dot{\xi} &= \beta \left(\frac{\partial H}{\partial q_i} F_i - T \frac{\partial F_i}{\partial q_i} \right). \end{aligned} \tag{27}$$

For the case $h_2 = F \equiv 0$, $h_1 = \zeta$ and $G_i = p_i$, the original Nosé-Hoover equations of motion are recovered. When these equations are ergodic, the time average of the non-Hamiltonian contributions to these equations of motion will be zero (i.e. $\langle h_1 \rangle = \langle h_2 \rangle = 0$). So in the cases of interest, the over all Hamiltonian character and the energy will be preserved on average.

If the system is ergodic, the initial conditions are irrelevant, unless the starting point is chosen in the set of measure zero for which the time evolution does not converge to the thermodynamic mean. Unfortunately it is not obvious how to determine whether the system is ergodic. In practice, the evaluation of distributions over various initial conditions should be sufficient. Aside from the initial conditions, there are two free parameters α and β, to be discussed in the next section. Whatever the functional choice of h_1 and h_2, their thermal distributions will be given by the exponent of their integrals. These integrals g_1 and g_2 must provide a normalizable distribution function f as given in (19). A nice feature of the original Nosé-Hoover equations (12) is that there are no fixed points. However, since fixed points will be present in more general situations, it is wise to avoid obvious stable fixed points in the general case (27). For simple functions F and G this can be done easily.

Analogous to the Nosé-Hoover oscillator, it is easily verified that the system of equations (27) conserves the pseudo-energy defined by

$$\mathcal{E} = H(q,p) + \frac{1}{\alpha} g_1(\zeta) + \frac{1}{\beta} g_2(\xi) + T \int_0^t \left[h_1(\zeta;t') \frac{\partial G_i}{\partial p_i} + h_2(\xi;t') \frac{\partial F_i}{\partial q_i} \right] dt'. \quad (28)$$

By direct substitution of the equations of motion (27) into $\dot{\mathcal{E}}$ it is easily checked that $\dot{\mathcal{E}} = 0$. The argument of the integral is precisely the divergence of the equations of motion with an overall negative sign:

$$\sum_{i=1}^{N} \left(\frac{\partial \dot{q}_i}{\partial q_i} + \frac{\partial \dot{p}_i}{\partial p_i} \right) = -T \sum_{i=1}^{N} \left[h_1(\zeta;t') \frac{\partial G_i}{\partial p_i} + h_2(\xi;t') \frac{\partial F_i}{\partial q_i} \right]. \quad (29)$$

For Hamiltonian systems the r.h.s. vanishes identically.

3. ONE- AND TWO-DIMENSIONAL EXAMPLES

Of main interest in canonical ensemble simulations is the non-equilibrium many body problem. Applying such methods blindly to complex systems is risky if we do not understand the limitations of these simulations. This can be achieved by studying the behavior of simple solvable one and two dimensional problems. In this section we consider a large class of one and two dimensional examples, contrasting our model to the predictions from the Nosé-Hoover approach, drawing special attention to convergence properties and limitations. These examples will provide insight into the more complex many body problem.

3.1 Equations of Motion

We have investigated our equations of motion (27) with a variety of interactions in one and two coordinate dimensions. In the space (q_i, p_i, ζ, ξ) (where $i = 1$ or $i = 1, 2$) the most general equations of motion we consider are

$$\begin{aligned} \dot{q}_i &= p_i - h_2(\xi) F_i, \\ \dot{p}_i &= -\frac{\partial V}{\partial q_i} - h_1(\zeta) G_i, \\ \dot{\zeta} &= \alpha \left(p_i G_i - T \frac{\partial G_i}{\partial p_i} \right), \\ \dot{\xi} &= \beta \left(\frac{\partial V}{\partial q_i} F_i - T \frac{\partial F_i}{\partial q_i} \right). \end{aligned} \tag{30}$$

Here the Hamiltonians are of the form $H = \sum_i p_i^2/2 + V(q)$, and the functions $F_i = F_i(q,p)$ and $G_i = G_i(q,p)$ are general functions of all coordinates and momenta. For one dimensional systems, the potential energy $V(q)$ has been taken as that of a harmonic oscillator, symmetric double well, or antisymmetric well:

$$V(q) = \frac{1}{2} q^2, \qquad V(q) = \frac{1}{2}(q^2 - 1)^2, \qquad V(q) = \begin{cases} \frac{1}{2}(q^2 - 1)^2, & \text{if } q \geq 0; \\ \frac{1}{2}(1 - q^3), & \text{if } q < 0. \end{cases} \tag{31}$$

In Posch *et al*'s detailed study of the Nosé-Hoover equations, a periodic 2-d potential was investigated [5] . This provided evidence that the method works for more complicated systems. However, in general, characteristic failures in 1-d are evidenced in 2-d systems. We have studied the general non-periodic potential

$$V(q_1, q_2) = a_1 q^4 + a_2 q^2 + a_3 q_1^2. \tag{32}$$

For various choices of a_i this potential produces a mexican hat, a symmetric double well or a transition between the two. Especially for low temperatures,

the harmonic oscillator behavior of the potential near the minimum prevents the Nosé-Hoover equations form thermalizing and reproducing the canonical ensemble.

For all these Hamiltonians, we have achieved rapid convergence of the canonical ensemble averages, to be described below. A wide variety of forces F_i and G_i have been considered:

$$F_i(q,p),\ G_i(q,p) = \begin{cases} 0 \\ q_i^n p_i^m, \\ \cos\left(q_i^n p_i^m\right) \\ \exp\left(q_i^n p_i^m\right)/2 \end{cases} \qquad \text{for } n,m = 0,1,2,3,4. \tag{33}$$

For the couplings to the thermal bath, we have selected

$$h_1(\zeta) = \begin{cases} \zeta^n, & n = 1,3 \\ \zeta|\zeta|, \end{cases} \qquad h_2(\xi) = \begin{cases} \xi^n, & n = 1,3 \\ \xi|\xi|, \end{cases} \tag{34}$$

The number of combinations provides a multitude of equations of motion, for which we have investigated the convergence and chaotic behavior, dependence on the initial conditions and the parameters α and β. There is one caveat: These functions must be chosen in such a way as to avoid the presence of stable fixed points in the equations of motion, which can destroy the ergodicity.

3.2 Generalized Couplings and the Cubic Coupling Scheme

In choosing the general thermal bath coupling functions h_1, h_2, F_i and G_i, the equations of motion no longer retain the previous simple 'physical' interpretations provided by Nosé and Hoover. But the fact that we do not follow Nosé's proof of the equivalence of the canonical and microcanonical ensembles is not important. By the construction of the equations of motion and the choice of the phase space probability distribution $f(q,p,\zeta,\xi)$, we will naturally reproduce the canonical distributions providing we have ergodic behavior.

The preferred couplings we shall illustrate mostly throughout these examples are explicitly

$$\begin{aligned} \dot{q}_i &= p_i - \xi q_i^3, \\ \dot{p}_i &= -\frac{\partial V}{\partial q_i} - \zeta^3 p_i, \\ \dot{\zeta} &= \alpha(p^2 - NT), \\ \dot{\xi} &= \beta(\sum_{i=1}^{N} \frac{\partial V}{\partial q_i} q_i^3 - 3Tq^2), \end{aligned} \tag{35}$$

with $p^2 = \sum_{i=1}^{N} p_i^2$ and $q^2 = \sum_{i=1}^{N} q_i^2$. These equations do not have any stable fixed points. To see this consider the linearization of these equations. Define the vector

$$\phi = (q_1, ..., q_N, p_1, ..., p_N, \zeta, \xi), \tag{36}$$

and denote by ϕ_i the $i-th$ element of the vector. The equations of motion (35) can be cast in the form:

$$\dot{\phi} = \mathcal{F}(\phi), \tag{37}$$

where $\mathcal{F}(\phi)$ represents the right hand side of (35). At an arbitrary point ϕ along the flow, the equations can be linearized and the eigenvalues studied. This establishes a general picture of the divergence of neighboring trajectories and the presence of chaos. The trace of the stability matrix $\frac{\partial \mathcal{F}}{\partial \phi}$ can be seen to be

$$\mathrm{Tr}\,\frac{\partial \mathcal{F}}{\partial \phi} = -3\xi q^2 - N\zeta^3. \tag{38}$$

The fixed point (F.P.) condition from the equations of motion (35) can be written as

$$\begin{aligned} p_i &= \xi q_i^3, \\ \frac{\partial V}{\partial q_i} &= -\zeta^3 p_i, \\ p^2 &= NT, \\ \sum_{i=1}^{N} p_i \frac{\partial V}{\partial q_i} &= 3T\xi q^2. \end{aligned} \tag{39}$$

The first three equations of (39) can be used and equated to the fourth equation in (39) to yield the relation

$$3\xi q^2 = -\zeta^3 N. \tag{40}$$

(We have used the fact that $\xi \neq 0$, since clearly there is no fixed point for $\xi = 0$ at any non-zero temperature.) Comparing to the trace (38) we find that the sum of the eigenvalues λ_i of $\frac{\partial \mathcal{F}}{\partial \phi}$ is identically zero for an arbitrary potential (in any dimension) in this coupling scheme at the fixed point:

$$\mathrm{Tr}\,\frac{\partial \mathcal{F}}{\partial \phi}\bigg|_{\mathrm{F.P.}} = \sum_i \lambda_i \equiv 0. \tag{41}$$

Hence there are no stable fixed points. This coupling, which will be referred to as the cubic coupling scheme, provides ergodic behaviour in all the examples we

have studied. The (unnormalized) thermal distributions in this scheme follow from (19)

$$\begin{aligned} f(p_i) &= e^{-p_i^2/2T}, \qquad f(\zeta) = e^{-\zeta^2/2T\alpha}, \\ f(q_1,...,q_N) &= e^{-V(q)/T}, \qquad f(\xi) = e^{-\xi^4/4T\beta}. \end{aligned} \tag{42}$$

The numerical evidence of ergodicity is based on the independence of initial conditions on the final thermal distributions, and will be discussed after some examples are presented.

3.3 Phase Space Evolution

How does this method actually work? This is easily illustrated by example. Consider the 2-d double well potential

$$V(q_1,q_2) = q^4 + q^2 - 3q_1^2, \tag{43}$$

where $q^2 = q_1^2 + q_2^2$ and $q^4 = (q^2)^2$. This well has two minima located along the q_1 axis at $(q_1,q_2) = (\pm 1, 0)$ with a barrier height of 1. Consider the trajectories in this potential at a temperature $T = 1$ in the cubic coupling scheme. A selection of 2-d projected phase spaces are illustrated in Fig. 1 after plotting 10^3 points. The trajectory has been sampled every $dt = 0.02$, which corresponds to a time $t = 20$, where $t = 1$ is the characteristic time of the system.[1] In this specific example, the initial condition is

$$\phi_0 = (q_1,q_2,p_1,p_2,\zeta,\xi)_0 = (0.2, 0.21, -0.3, -0.37, 0, 0). \tag{44}$$

However, the system is ergodic, and thus the particular initial conditions are irrelevant. There is no apparent regularity in the trajectories at this time. After 5000 points, and a time $t = 100$, the phase space projections already begin to appear quite dense, as seen in Fig. 2. The double well structure is quite evident in the phase space sections that include q_1. The resulting distributions that correspond to $t = 100$ are shown in Fig. 3 (histograms) and can be seen to agree quite well with exact thermodynamic averages (solid curves), given in Eq. (42). Using the specific form of V from Eq. (43), we obtain

1 In the numerical simulations, integration of the equations of motion was performed using the IMSL subroutine DIVPRK, with an error tolerance of $10^{-6} - 10^{-9}$. The dt referred to throughout the text is the sample time, which is in general larger than the actual integration step, determined by the subroutine. All computations were performed in double precision on a VAX 3100 workstation.

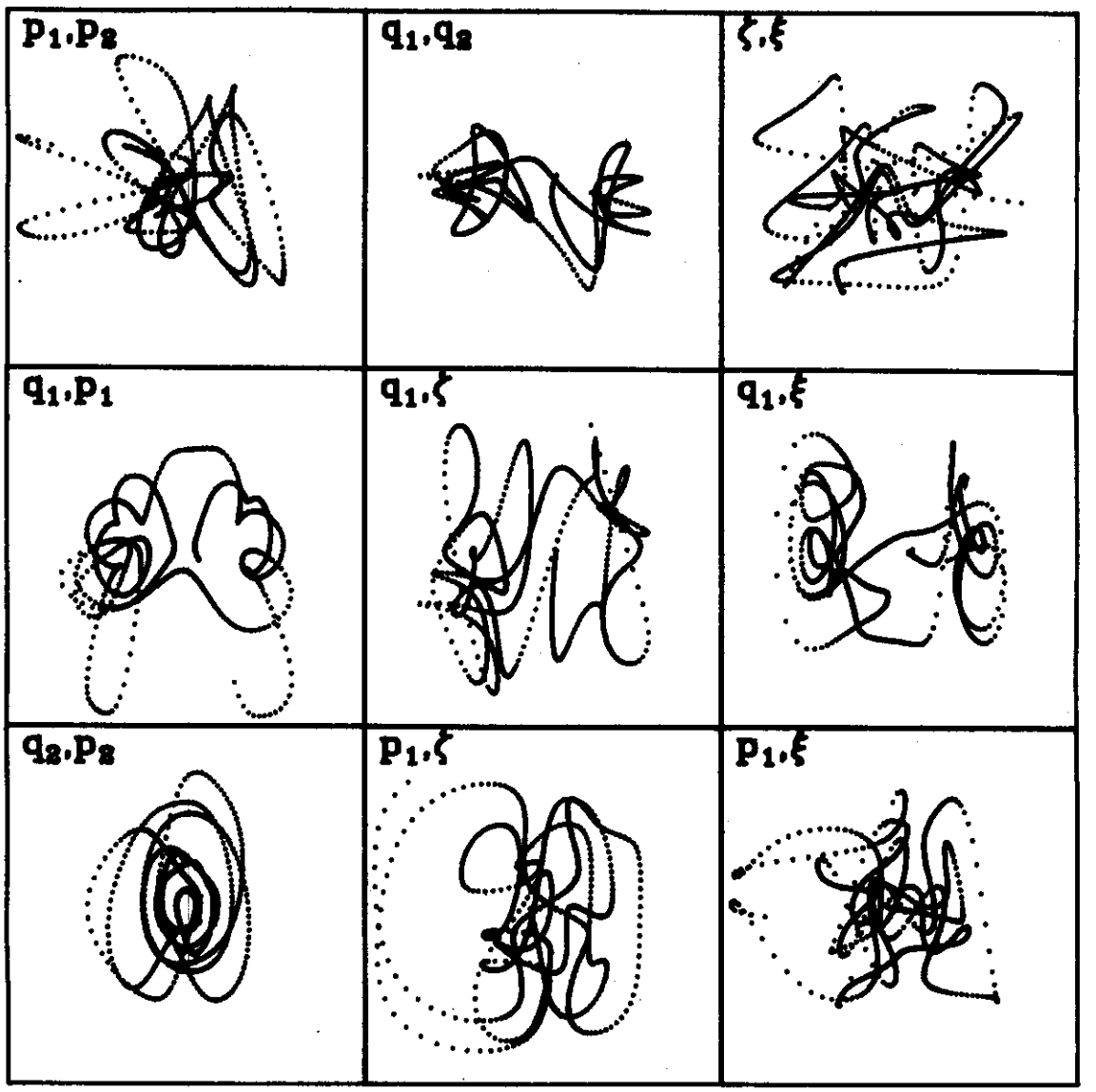

FIGURE 1. Projections of a trajectory for the 2-d double well potential (43) using the initial condition (44) with $\alpha = \beta = T = 1$ in the cubic coupling scheme. The trajectory has been sampled every $dt = 0.02$ for a total duration of $t = 20$ (1000 points). The limits in the figure are $-4 \leq p_1, p_2, \xi \leq 4$ and $-2.5 \leq q_1, q_2, \zeta \leq 2.5$.

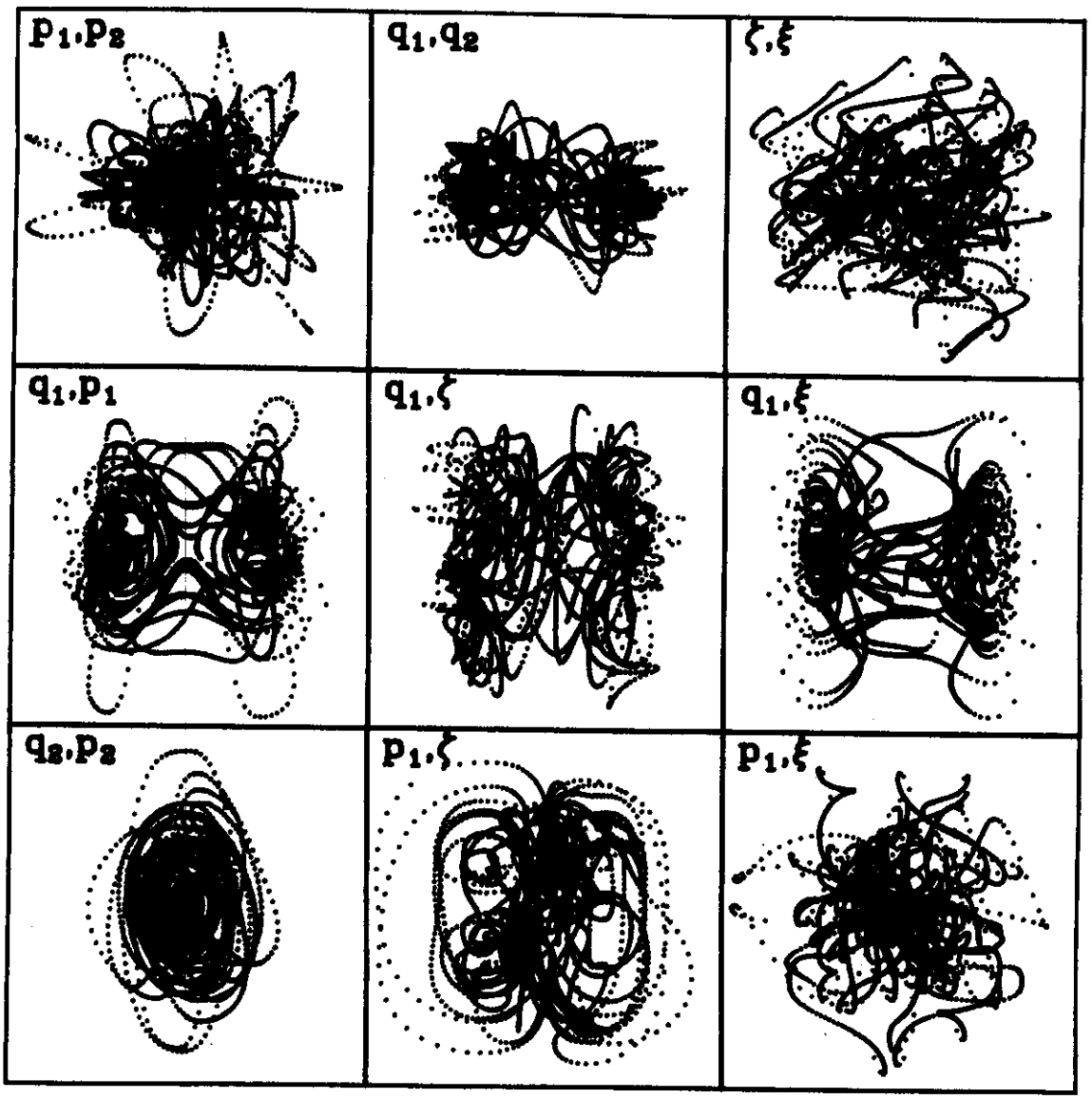

FIGURE 2. Same as Fig. 1 but with $t = 100$ (5000 points).

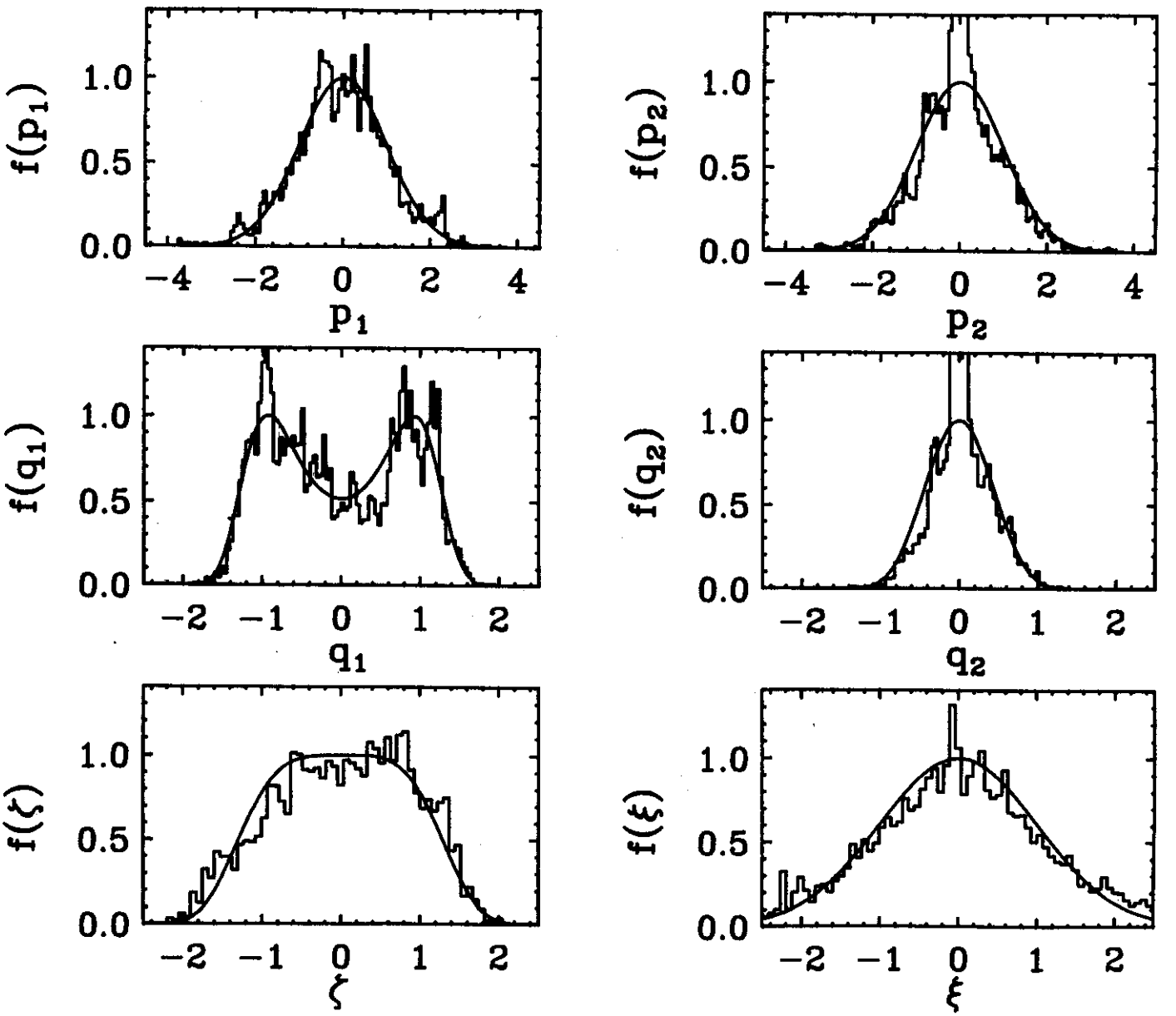

FIGURE 3. Thermal distributions corresponding to the trajectory in Fig. 2. In this and all subsequent figures the numerical results are represented by histograms, and the number of bins in the histogram is 100. The exact distributions are represented by smooth curves.

$$f(q_1) = e^{-(4q_1^4-20q_1^2-1)/8T}\sqrt{2q_1^2+1}\,K_{\frac{1}{4}}\left(\frac{(2q_1^2+1)^2}{8T}\right),$$
$$f(q_2) = e^{-(q_2^4+4q_2^2-1)/2T}\sqrt{|q_2^2-1|}\,K_{\frac{1}{4}}\left(\frac{(q_2^2-1)^2}{2T}\right), \tag{45}$$

where $K_{1/4}$ is the Macdonald function. The histograms are obtained by binning each point in the time evolution of the classical trajectory in the extended phase space. The small irregularities in the $f(q_2)$ and $f(p_2)$ distributions vanish at longer times, as shown in Fig. 4, which corresponds to $t = 2000$. This coupling scheme turns out to converge independently of initial conditions almost everywhere (that is, aside from the obvious point $p_i = q_i = 0$ at $t = 0$). This can be shown by taking a random sampling of initial conditions.

Dense phase space portraits are not sufficient to determine whether or not the equations will provide canonical ensemble averages. As mentioned before, recurrent trajectories can also produce a (non-ergodic) dense phase space distribution. Consider the 1-d quartic potential at $T = 1$ in the Nosé-Hoover scheme with initial condition $(q_0, p_0, \zeta_0) = (1.3, 0, 0)$ and $\alpha = 1$. Evolving these equations a long time to $t = 10^4$ (corresponding to 5×10^5 time steps of $dt = 0.02$), the thermal distributions can be checked to have converged. Again, the characteristic time of the Hamiltonian is $t = 1$. The projected 2-d phase spaces appear dense, as shown in Fig. 5. However, the thermal distributions have converged to the incorrect results (Fig. 6), indicating recurrent rather than ergodic behavior. The exact thermal distributions in this case are

$$f(p) = e^{-p^2/2T}, \qquad f(q) = e^{-(q^2-1)^2/2T}, \qquad f(\zeta) = e^{-\zeta^2/2T}. \tag{46}$$

In the cubic coupling scheme, the phase space portraits (at the same time) look identical to those in Fig. 5, but the thermal distributions have converged to the proper result as indicated in Fig. 7. This corresponds to initial condition $(q_0, p_0, \zeta_0, \xi_0) = (1.3, 0, 0, 0)$ and $\alpha = \beta = 1$. The cubic coupling is evident in the thermal distribution for ξ which has the form of $\exp(-\xi^4/4T)$ (see Eq. (42)). Hence one cannot judge the outcome of an application of this method as being accurate simply on phase space projections alone.

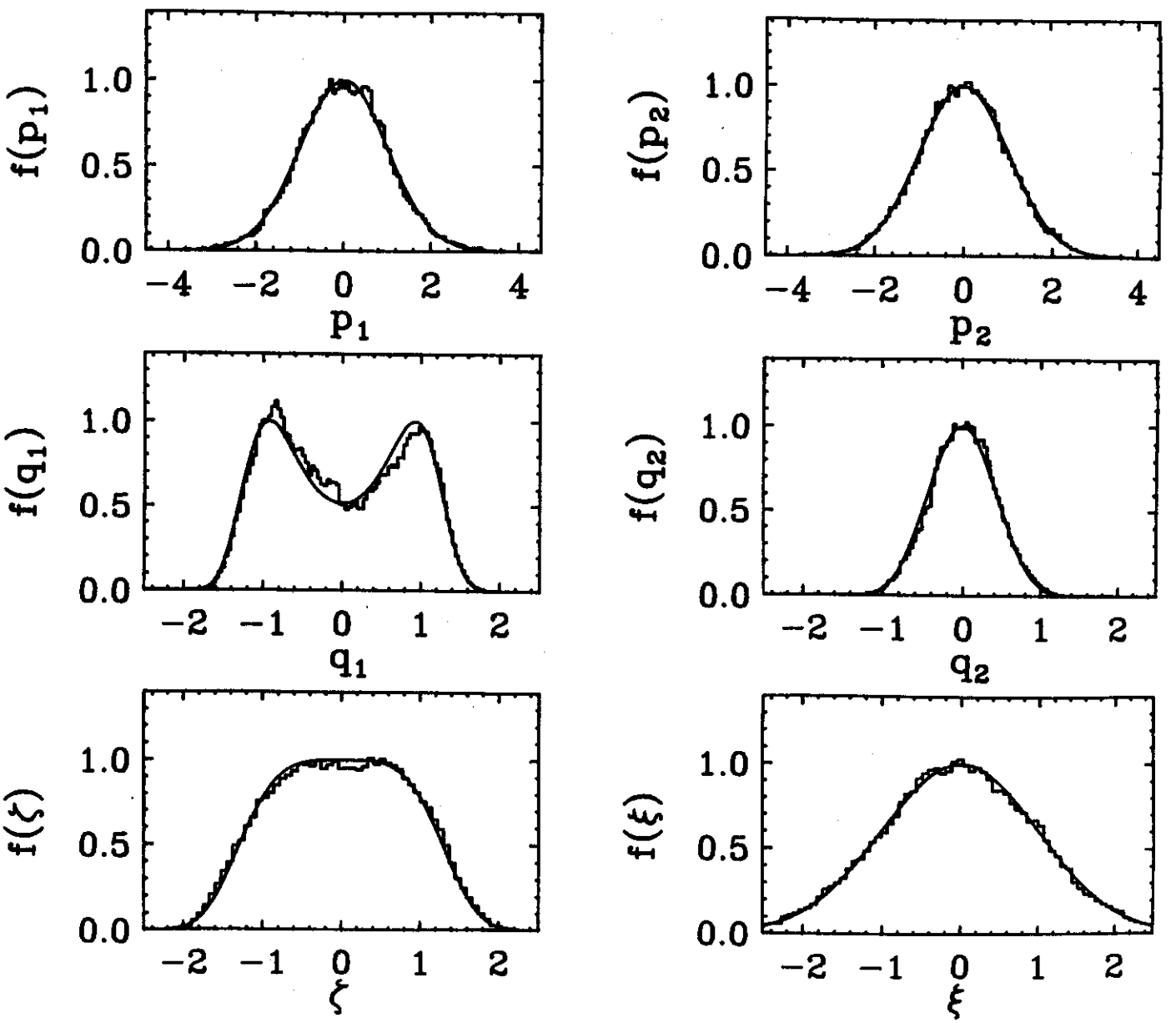

FIGURE 4. Same as Fig. 3 but with $t = 2000$. The small deviations have a statistical origin.

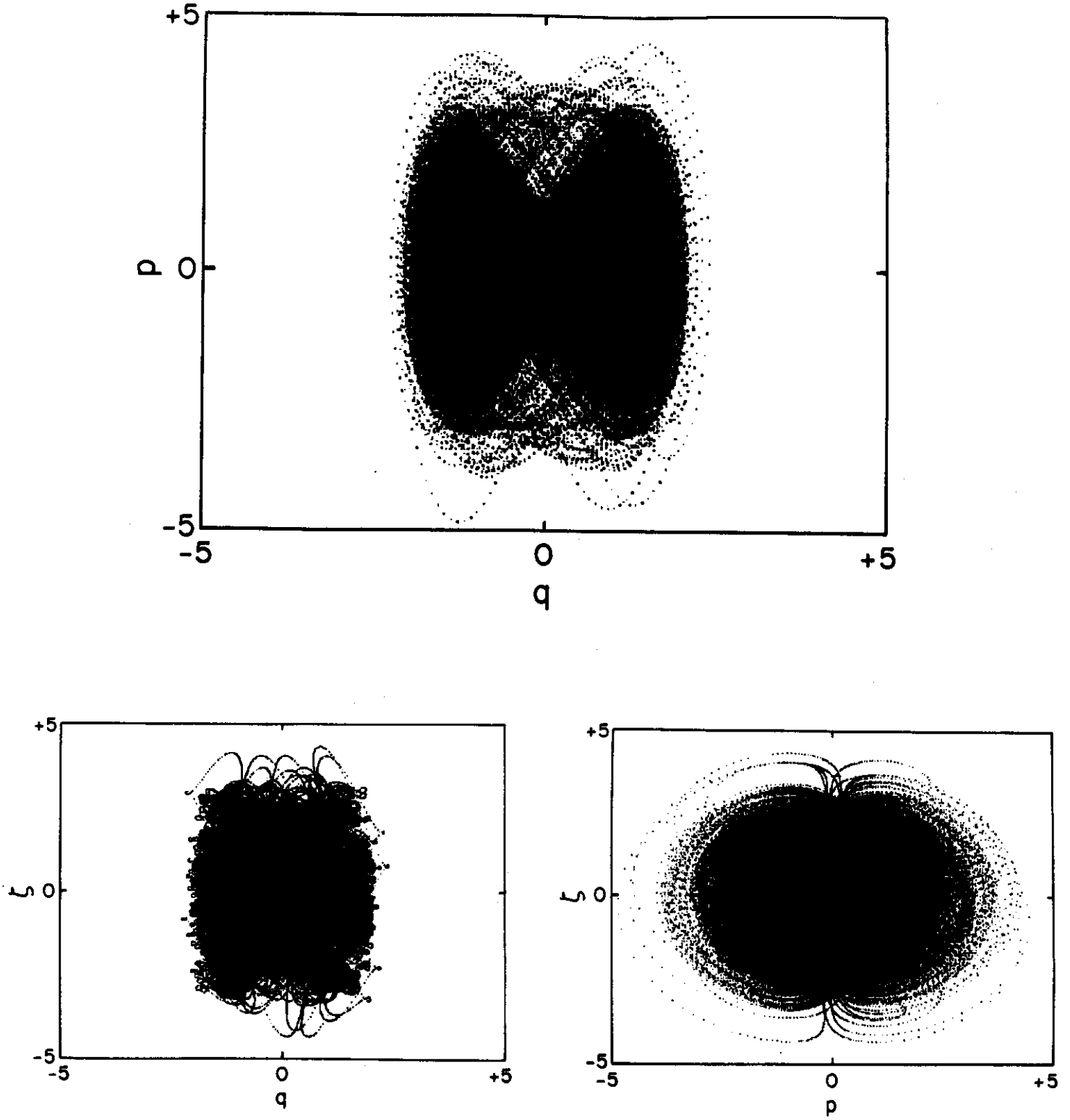

FIGURE 5. Dense phase space projections for a 1-d quartic potential, with initial conditions $(q_0, p_0, \zeta_0) = (1.3, 0, 0)$ in the Nosé-Hoover model with $\alpha = T = 1$, after 5×10^5 steps at $dt = 0.02$.

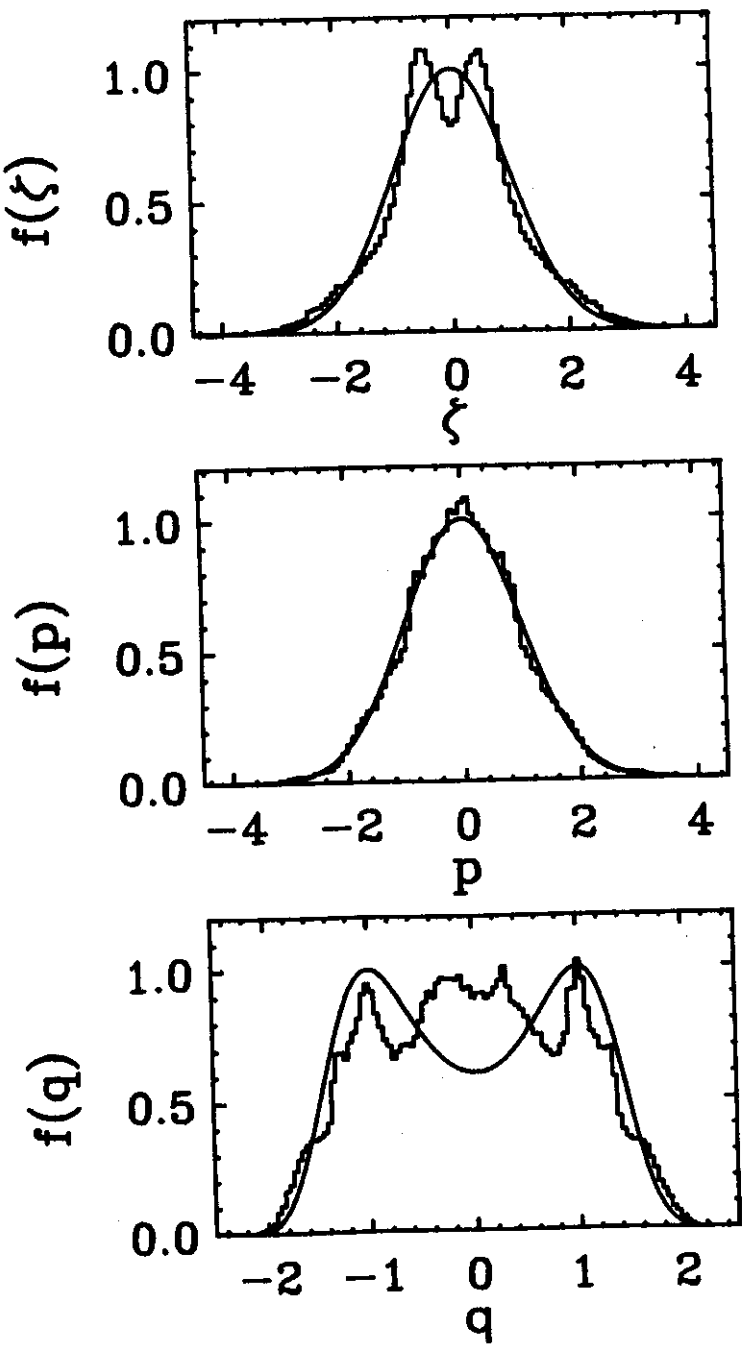

FIGURE 6. Converged Nosé-Hoover thermal distributions corresponding to the dense phase space in Fig. 5.

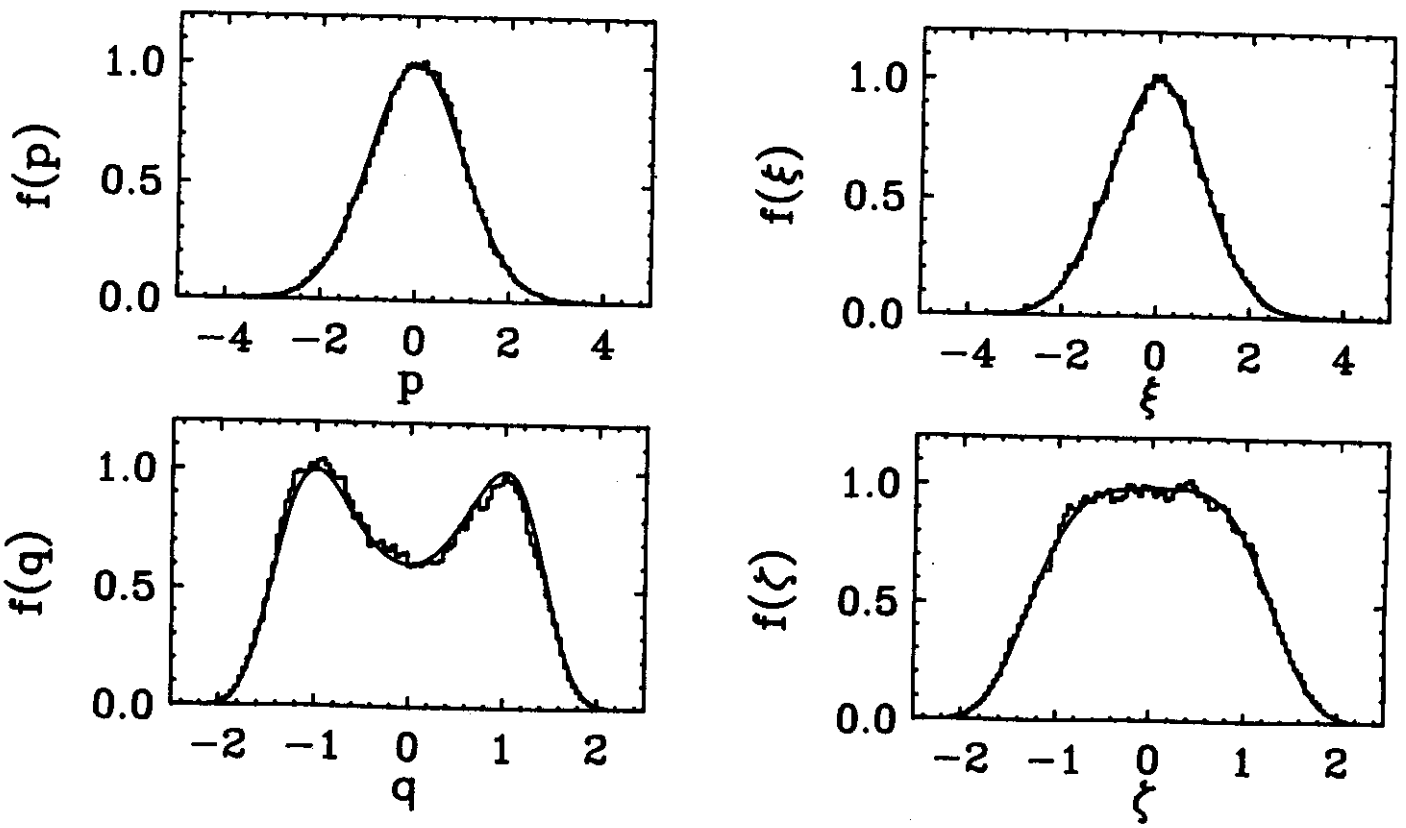

FIGURE 7. Converged thermal distributions for the 1-d quartic potential using the cubic coupling scheme with $\alpha = \beta = T = 1$.

3.4 Temperature Dependence

Chaoticity of the equations of motion can depend strongly on the temperature. Although such problems have not been seen in the cubic coupling scheme, they are easily found in the Nosé-Hoover scheme. As an example, consider the asymmetric potential of (31), with the initial condition $(q_0, p_0, \zeta_0) = (0.4, -0.34, 0.5)$ and $\alpha = 1$. Fig. 8a shows the good agreement obtained at $T = 1$. The phase space (q,p) (not displayed) is densely filled and the thermal distributions are in excellent agreement with the exact result. By changing the temperature to $T = 0.1$, the results are completely different, as indicated in Fig. 8b. The phase space still appears dense, whereas the thermal distributions converge to incorrect functions. At even lower temperatures, the agreement becomes progressively worse. In the cubic coupling scheme, the convergence to the exact result has been checked down to temperatures of 10^{-4}, for which there is excellent agreement, as illustrated in Figs. 9. From our simulations, optimum values for the coupling strengths seem to be $\alpha = 1/T$ and $\beta = 1/T^2$.

3.5 Examples in 2-d

The cubic coupling scheme seems to provide ergodic trajectories in a variety of cases. The results of a simulation with a mexican hat potential in 2-d is shown in Fig. 10, where

$$V(q_1, q_2) = q^4 - q^2. \tag{47}$$

Here $q^2 = q_1^2 + q_2^2$, and the corresponding exact thermal distribution for q_i is

$$f(q_i) = e^{-(4q_i^4 - 4q_i^2 - 1)/8T} \sqrt{|2q_i^2 - 1|} K_{\frac{1}{4}} \left(\frac{(2q_i^2 - 1)^2}{8T} \right). \qquad (i = 1, 2) \tag{48}$$

The simulation was carried out at a temperature $T = 0.1$, using $5 \cdot 10^5$ time steps, $dt = 0.01$ resulting in a total time $t = 5000$. The mexican hat structure is clear form the thermal distributions of q_1 and q_2, as well as the exponential quadratic and quartic distributions for ξ and ζ. By breaking the rotational symmetry, we can study the 2-d double well potential

$$V(q_1, q_2) = q^4 + q^2 - 3q_1^2, \tag{49}$$

illustrated in Fig. 11 (see also Sec. 3.3). As before $T = 0.1$, $dt = 0.01$ and $t = 5000$. The exact thermal distributions are given in Sec. 3.3. At this low

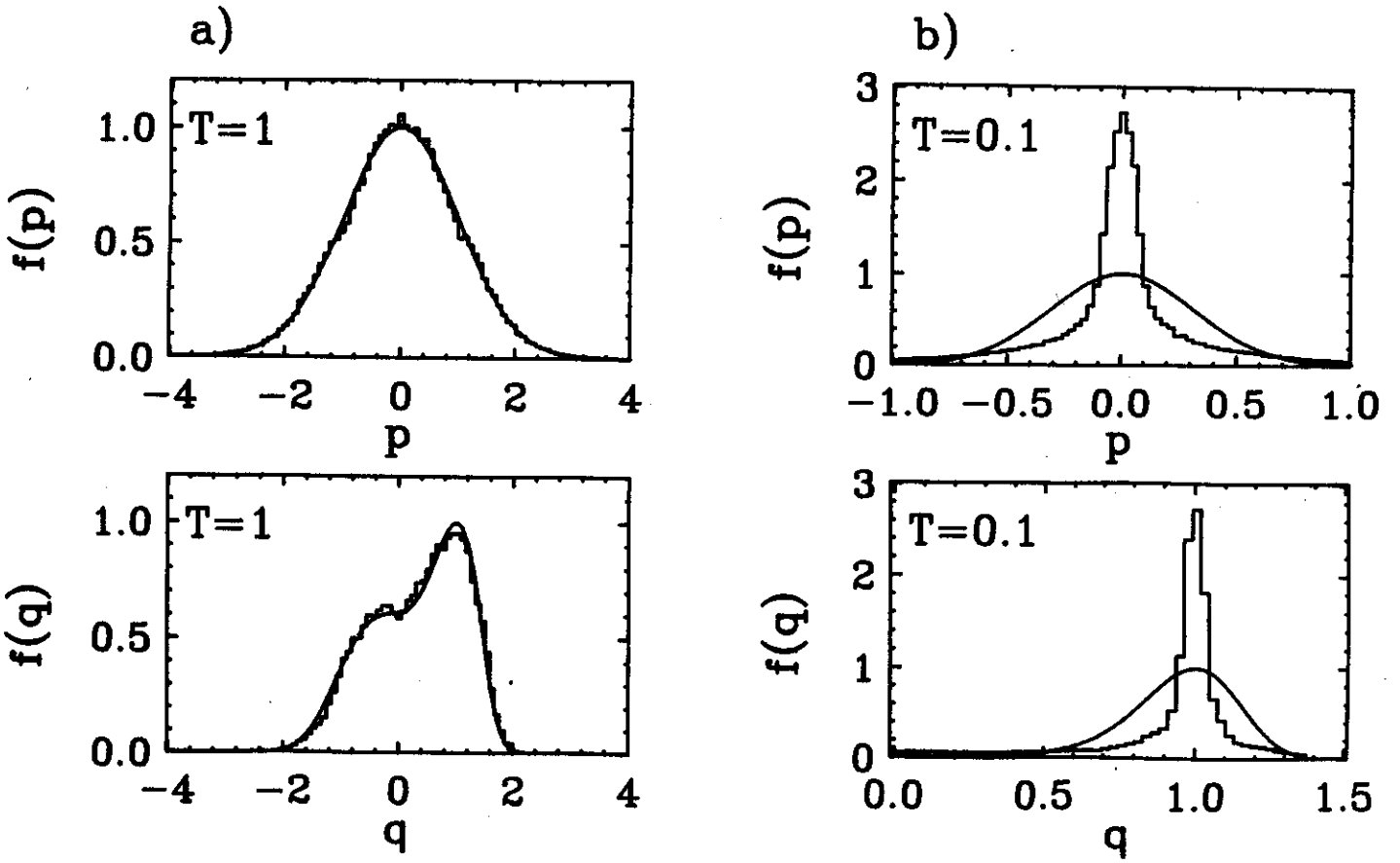

FIGURE 8. (a) Thermal distributions for a 1-d asymetric potential using initial conditions $(q_0, p_0, \zeta_0) = (0.4, -0.34, 0.5)$ and $\alpha = 1$ in the Nosé-Hoover model at $T = 1$. (b) Same as (a) but with $T = 0.1$. In both cases $\alpha = 1$.

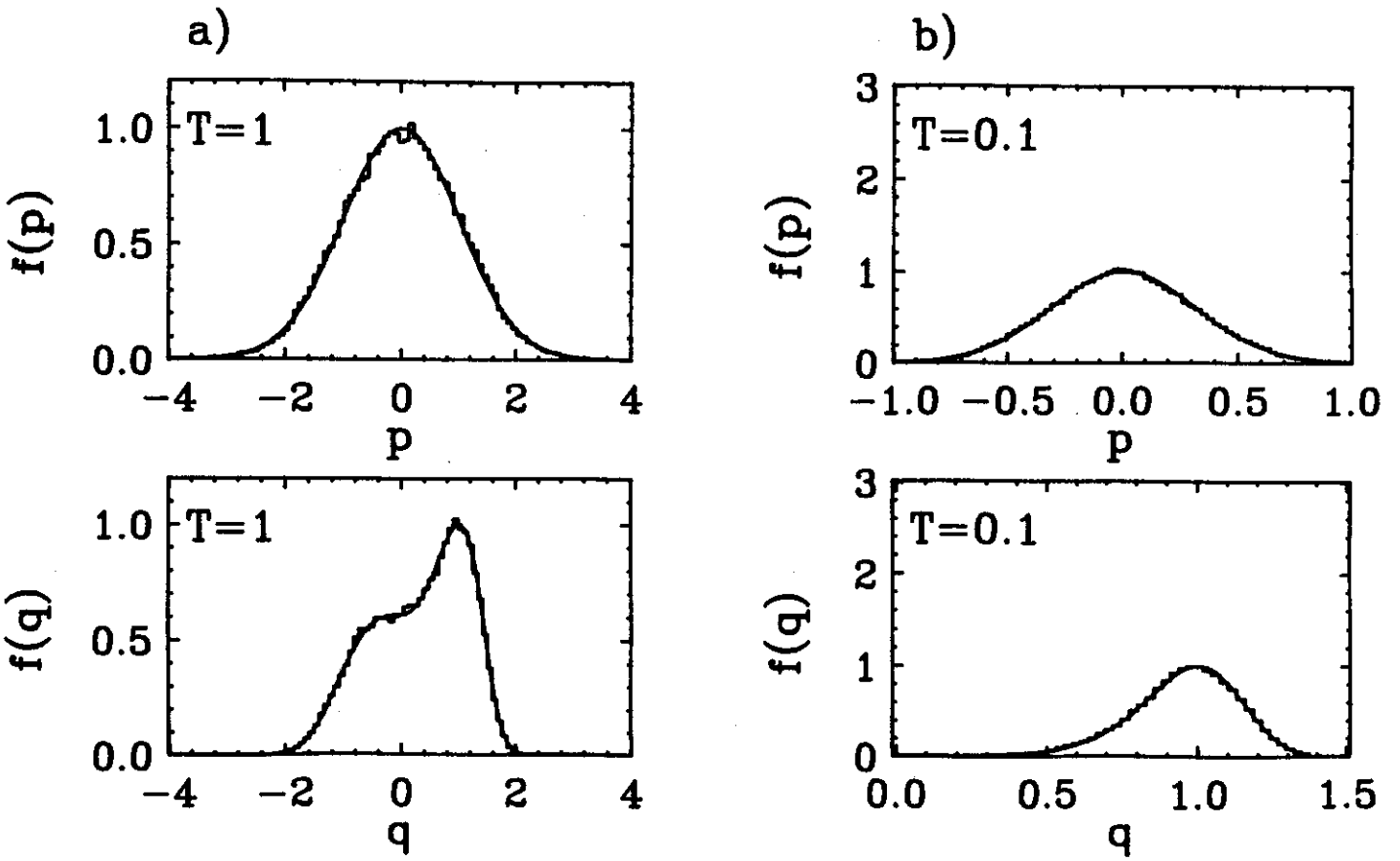

FIGURE 9. (a) Thermal distributions for a 1-d asymetric potential in the cubic coupling scheme with $\alpha = \beta = T = 1$. (b) Same as (a) but with $\alpha = \beta = 10$ and $T = 0.1$.

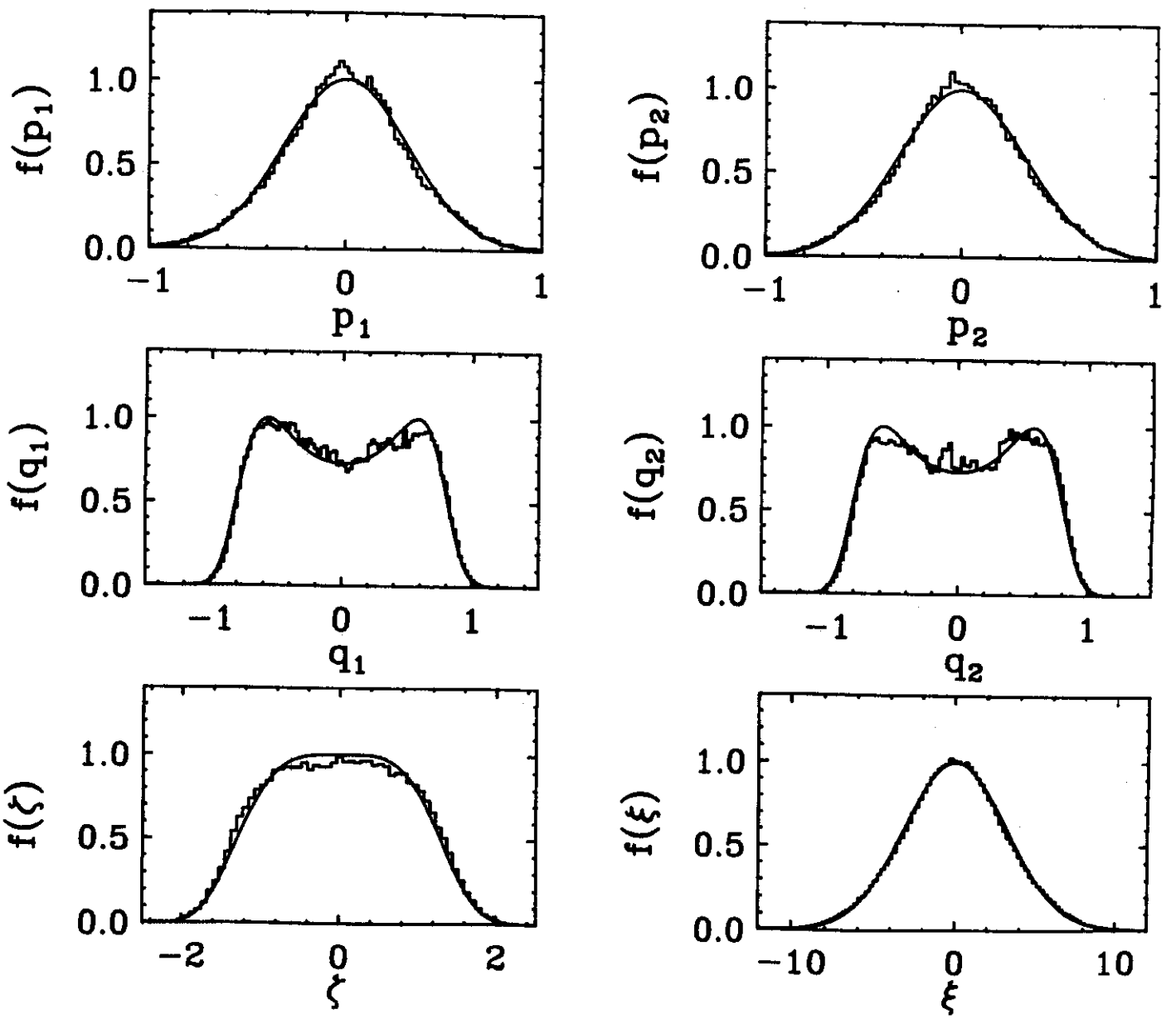

FIGURE 10. Exact thermal distributions (solid) compared to computed distributions (histograms) in a 2-d mexican hat potential at $T = 0.1$, $dt = 0.01$ and $t = 5000$ in the cubic coupling scheme with $\alpha = 10$ and $\beta = 100$.

temperature, the ratio of the maximum to the minimum of the $f(q_1)$ distribution is approximately 13400 : 1. Due to the classical tunneling probability, there is a large oscillation time scale for the trajectories between the two wells. On time scales that are smaller than this oscillation time, the ergodic trajectories reproduce the functional shape of the isolated potential well. On the longer time scale the oscillations will gradually reduce, eventually resulting in the exact result. The figure of $f(q_1)$ was taken when the trajectory had crossed into the other minimum and filled that side for a short time. In all these cases, the agreement is excellent.

3.6 Ergodicity and Convergence

Unfortunately there is no well defined procedure to determine whether or not the equations of motion, with a particular coupling to the thermal bath, are ergodic or simply recurrent. In order to determine this for the systems studied in this article, we have resorted to brute force methods. Ergodicity is checked for a particular model by discretizing the extended phase space and using each lattice site as an initial condition. The edges of the phase space are chosen by the condition that the exact thermal distribution along the edge is 10^{-4} of its maximum value. For each initial condition, the equations are evolved and the deviation of the computed distributions from the exact thermal distributions computed. For some extended phase space variable $\phi_k = q_i, p_i, \zeta, \xi$, we define the deviation at time t as (in percent)

$$\Delta(\phi_k, t) = 100 \int d\phi_k \; |f_{exact}(\phi_k) - f_{calc}(\phi_k, t)| \quad (\%), \tag{50}$$

where $f_{exact}(\phi_k)$ is the exact normalized thermal distribution of ϕ_k, and f_{calc} is the normalized result obtained from the numerical simulation of the trajectory in the time interval $[0, t]$. If the equations are ergodic, the deviation should be independent of initial conditions (almost everywhere).

The deviations $\Delta(\phi_k, t)$ were computed for 1-d potentials using 300 initial conditions in the phase space (q, p, ζ, ξ) and evolving the system with $T = 1$ and $\alpha = \beta = 1$. In Fig. 12 (left) the deviations for each initial condition for the 1-d harmonic oscillator are plotted, where the equations were evolved to $t = 500$ and sampled in time steps of $dt = 0.01$. All initial conditions result in convergence to within roughly seven percent of the exact thermal distributions within this time. In Fig. 12 (right) the deviations for the 1-d quartic oscillator are plotted. Again all deviations fall within roughly seven percent of the exact result, indicating ergodic trajectories produced in the cubic coupling scheme.

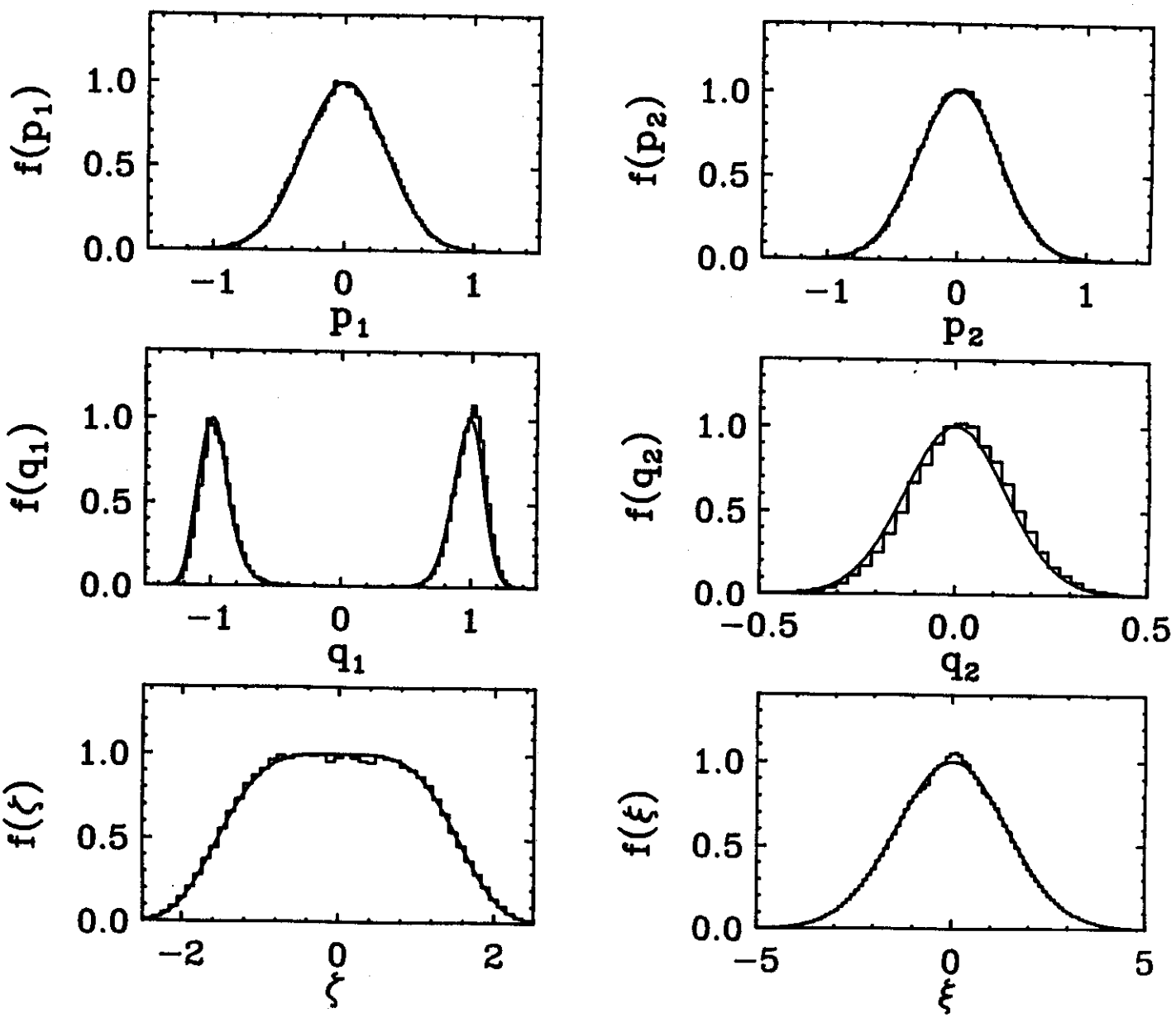

FIGURE 11. Exact thermal distributions (solid) compared to computed distributions (histograms) in a 2-d double well potential at $T = 0.1$, $dt = 0.01$ and $t = 5000$ in the cubic coupling scheme with $\alpha = \beta = 20$.

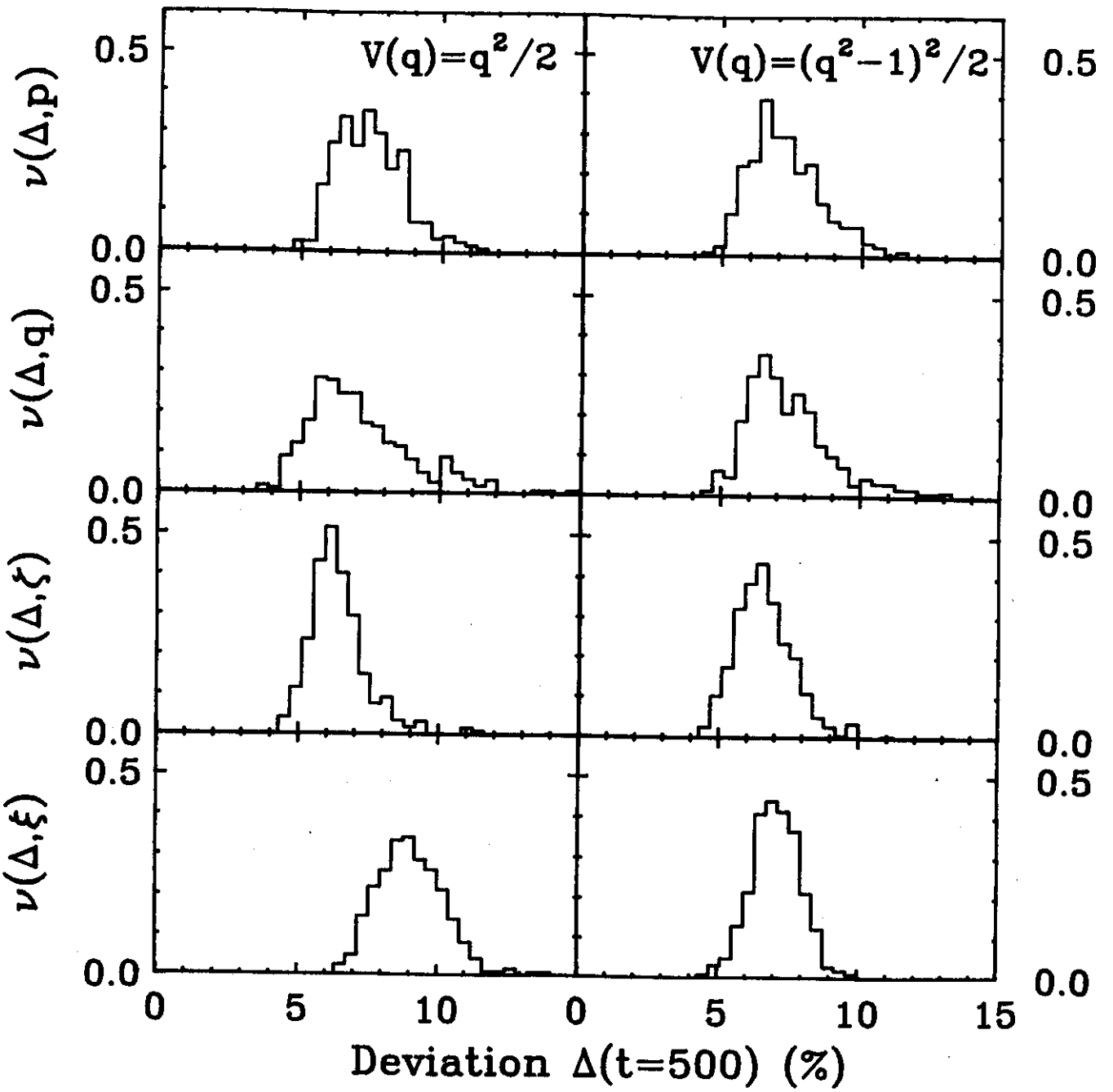

FIGURE 12. Normalized frequency distributions of deviations for 300 different initial conditions for the 1-d harmonic oscillator (left) and the 1-d quartic potential (right) in the cubic coupling scheme. The deviations are the integrated absolute difference of the exact and computed thermal distribution functions after following each trajectory to a time $t = 500$. In choosing these conditions we took the symmetry of the equations of motion into account.

The evolution of $\Delta(\phi_k, t)$ with time is an indication of the convergence time of the coupling scheme. Since the non-ergodicity of the harmonic oscillator potential has been the focus of attention in several studies, it is useful to compare its features with the cubic coupling scheme. This also provides the simplest example of one of the shortcomings of the Nosé-Hoover equations. Posch *et al* [5] have studied this system in depth and concluded, based on positive Lyapunov exponents and phase space plots, that there are chaotic regions of initial conditions in phase space. However, it is easily checked that the thermal distributions generated by choosing initial conditions from these chaotic regions do not converge to the canonical ensemble distributions for q, p or ζ. For the 1-d harmonic oscillator, the equations of motion are explicitly

$$\begin{array}{ll} \textit{Cubic Coupling} & \textit{Nosé} - \textit{Hoover} \\ \dot{q} = p - \xi q^3 & \dot{q} = p \\ \dot{p} = -q - \zeta^3 p & \dot{p} = -q - \zeta p \\ \dot{\zeta} = \alpha(p^2 - T) & \dot{\zeta} = \alpha(p^2 - T) \\ \dot{\xi} = \beta q^2(q^2 - 3T) & \end{array} \tag{51}$$

In the Nosé-Hoover scheme it is not always simple to determine regions of chaotic initial conditions. Posch *et al* [5] have found many sets of initial conditions leading to chaotic trajectories. For the initial conditions $(q_0, p_0, \zeta_0) = (0, 5, 0)$, a maximum Lyapunov exponent was found to correspond to $\alpha = 3$. An additional set of chaotic initial conditions for the harmonic oscillator is $(q_0, p_0, \zeta_0) = (0, 1.75, 0)$ and $\alpha = 10$ [5] . The time evolution of $\Delta(\phi_k, t)$ has been computed for these initial conditions, and is shown in Fig. 13. The relative deviations $\Delta(p, t)$, $\Delta(q, t)$ and $\Delta(\zeta, t)$ can be seen to converge rapidly to roughly 20%. The converged thermal distributions for the best fit ($(q_0, p_0, \zeta_0) = (0, 1.75, 0)$, $\alpha = 10$) are indicated in Fig. 14 at a time $t = 10^5$. In the cubic coupling scheme the rate of convergence of the deviations is the solid line in Fig. 13. In the same figure, the dashed line (drawn by hand) corresponds to $\Delta(\phi_k, t) \propto t^{-1/2}$, suggests that all remaining discrepancies between the computed and exact results have in this case only a statistical origin (N.B. the number of points is proportional to the time). In the cubic coupling scheme the deviations converge to the exact results as is illustrated in Fig. 15, using $\alpha = \beta = 1$ and $T = 1$. Once again we stress that while the results of Fig. 14 depend strongly on initial conditions, those of Fig. 15 are *independent* of initial conditions.

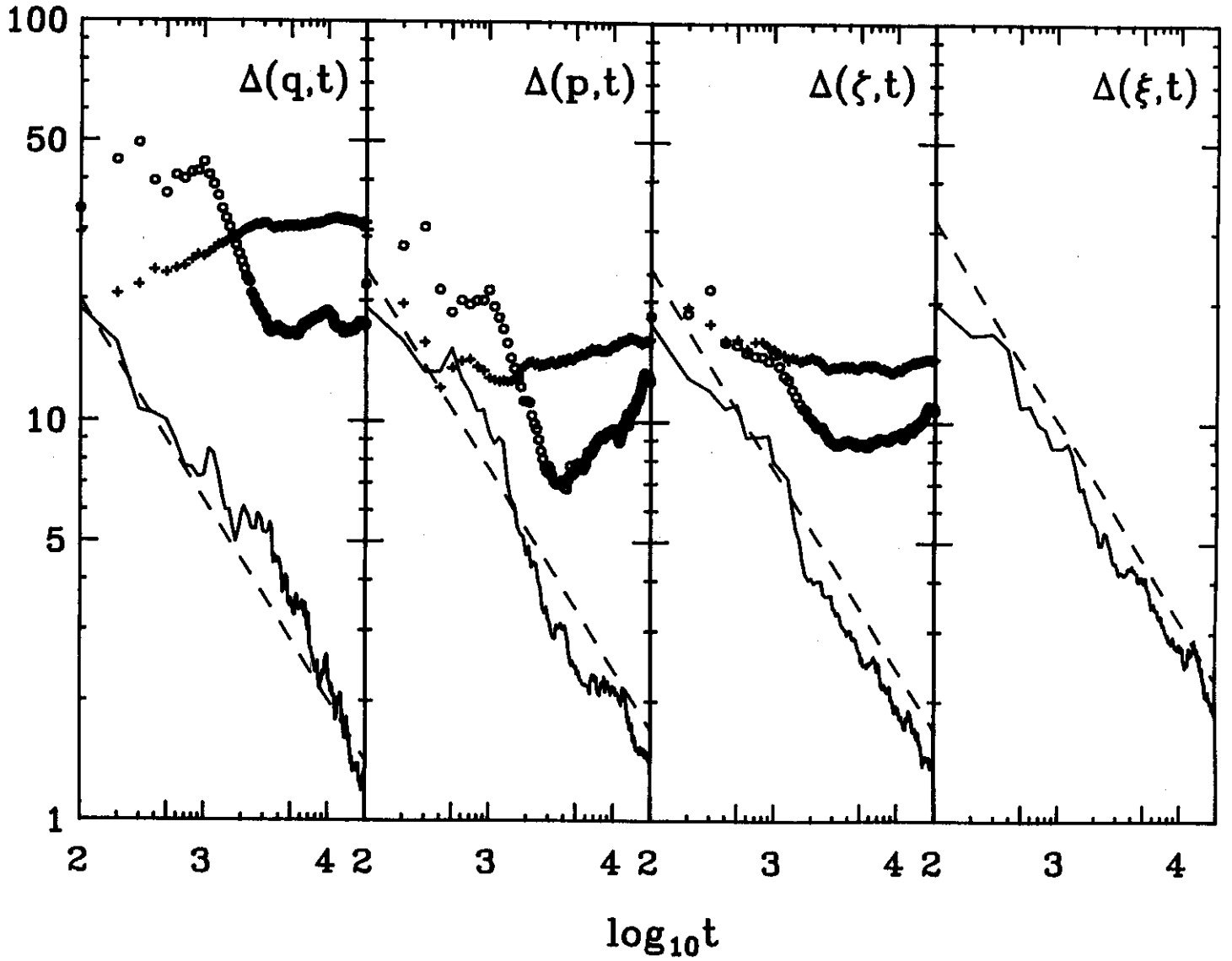

FIGURE 13. Time evolution of the relative deviations for the 1-d harmonic oscillator using chaotic initial conditions $(q_0, p_0, \zeta_0) = (0, 5, 0)$, $\alpha = 3$ (crosses), $(q_0, p_0, \zeta_0) = (0, 1.75, 0)$, $\alpha = 10$ (circles) in the Nosé-Hoover scheme, and in the cubic coupling scheme (solid line) with $\alpha = \beta = 1$. The dashed line corresponds to $\Delta(\phi_k, t) = const/t^{1/2}$, where the constant has been adjusted by eye.

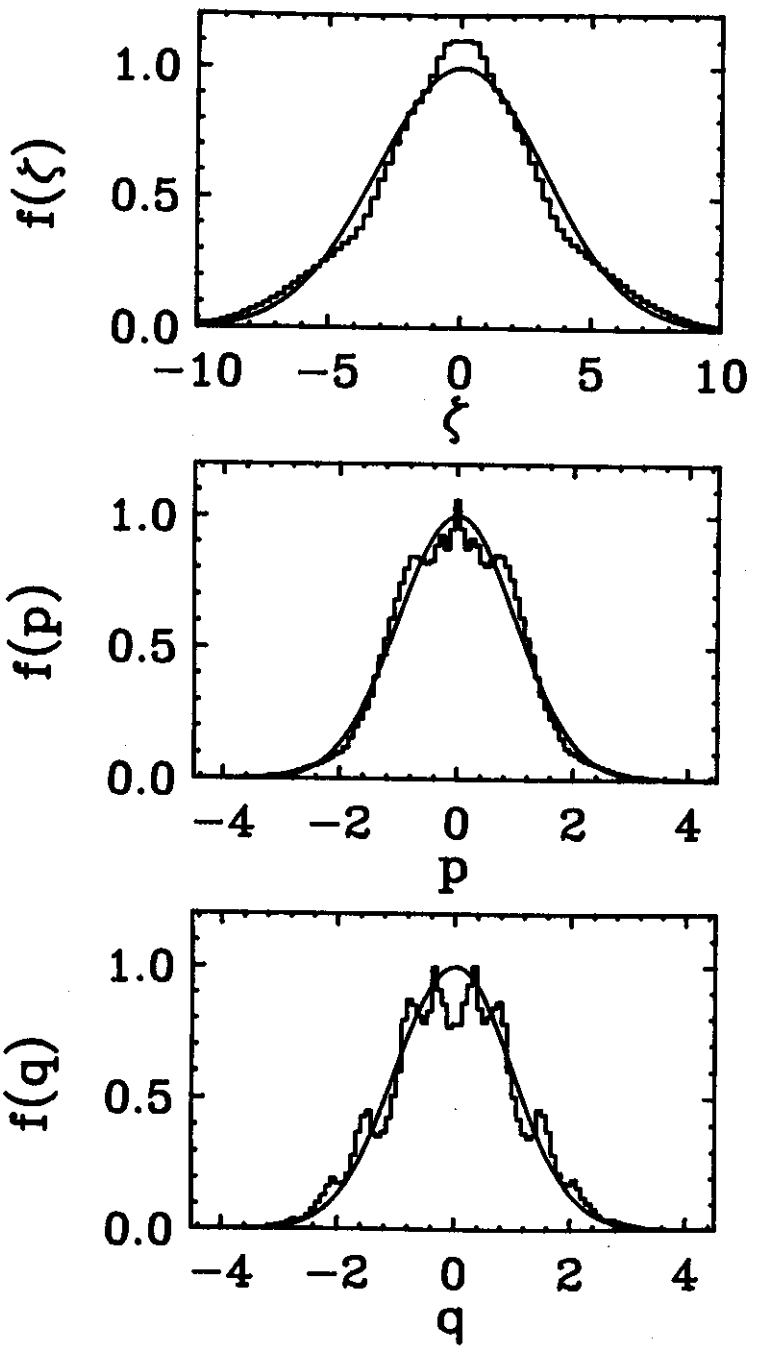

FIGURE 14. Converged thermal distributions $f(q)$, $f(p)$ and $f(\zeta)$ for the Nosé-Hoover harmonic oscillator with chaotic initial condition $(q_0, p_0, \zeta_0) = (0, 1.75, 0)$, $\alpha = 10$ and $T = 1$. The final time is $t = 10^5$ with $dt = 0.01$.

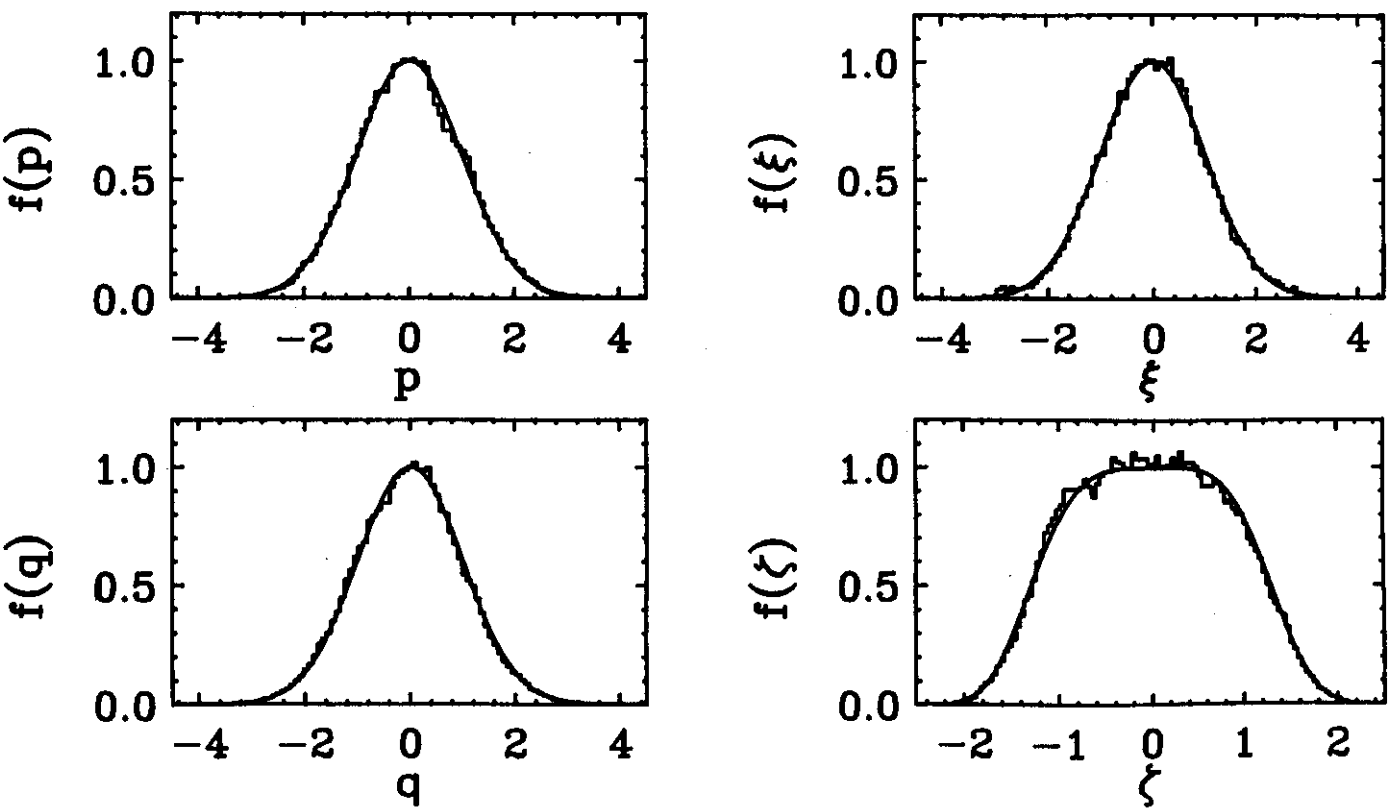

FIGURE 15. Converged thermal distributions $f(q)$, $f(p)$, $f(\zeta)$ and $f(\xi)$ for the cubic coupling scheme harmonic oscillator. The final time is $t = 5000$ with $dt = 0.01$.

3.7 Lyapunov Exponents

The maximum Lyapunov exponent measures the maximum divergence of neighboring trajectories in phase space. Positive exponents indicate exponential separation, whereas negative exponents indicate stability. In this way the exponents can indicate whether one should expect chaos or not. These exponents, however, do not guarantee ergodicity when positive, nor do they distinguish between ergodic or recurrent trajectories. Hoover computed these exponents for the 1-d harmonic oscillator in the Nosé-Hoover scheme [5] . Following standard techniques [9] , we consider two initial conditions in phase space separated by a distance ϵ. This vector is evolved in time with the linearized stability matrix (see Eqs. (36)-(37)):

$$\dot{\epsilon}_i = \frac{\partial \mathcal{F}_i}{\partial \phi_j}(t)\epsilon_j. \tag{52}$$

The formal solution is the time ordered product

$$\epsilon(t) = \hat{T} \exp \int_0^t dt' \frac{\partial \mathcal{F}_i}{\partial \phi_j}(t')\epsilon(0). \tag{53}$$

Then the maximum exponent is defined as

$$\lambda^{\max} = \lim_{n\to\infty} \frac{1}{n\tau} \sum_{i=1}^{n} \log |\epsilon(i\tau)|. \tag{54}$$

The maximum exponent for the 1-d harmonic oscillator potential at $T = 1$ is indicated in Fig. 16 for the Nosé-Hoover (crosses) and cubic coupling (circles) schemes. In the latter we have taken the additional restriction that $\alpha = \beta$. Although both examples of $\lambda^{\max}$ are positive, the smaller exponents (Nosé-Hoover) correspond to recurrent equations whereas the larger (cubic coupling) to ergodic equations. It is not completely clear how these exponents can provide relevant information to the central questions of ergodicity. However, it seems plausible that the Lyapunov exponent should be on the same scale or larger than the characteristic inverse time of the system under investigation in order to obtain ergodicity. On a similar note, Poincaré sections do not seem to offer any assistance in this respect.

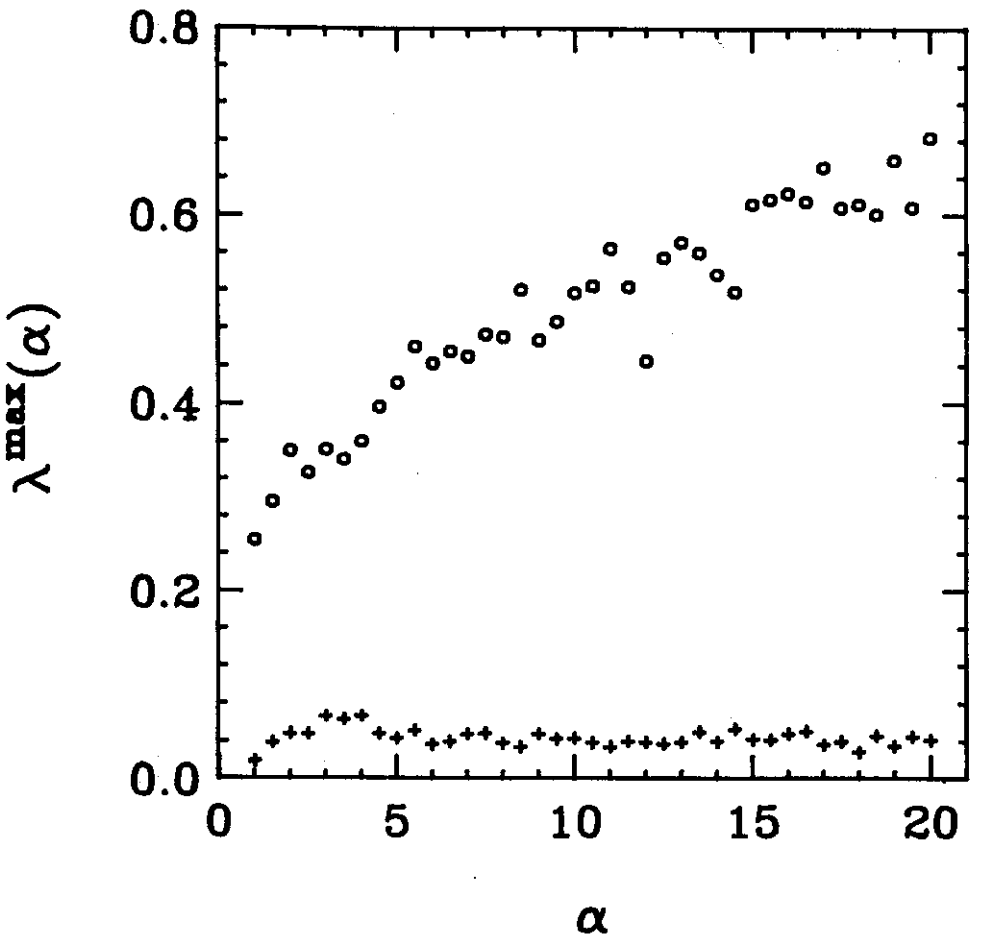

FIGURE 16. Maximum Lyapunov exponent for the Nosé-Hoover 1-d harmonic oscillator (crosses) using the initial conditions $(q_0, p_0, \zeta_0) = (0, 5, 0)$ as a function of the parameter α and for the cubic coupling scheme (circles) with $\alpha = \beta$, both at $T = 1$.

3.8 MIXING

The degree of distortion or mixing produced by the cubic coupling scheme can be illustrated by using a circle as an initial condition and examining its time evolution. In Fig. 17(a-b), a circle of 1000 equally spaced points is evolved for the harmonic oscillator, in the cubic scheme (with $\alpha = \beta = 1$) and in the Nosé-Hoover scheme ($\alpha = 3$), respectively. The characteristic period of the harmonic oscillator is $t = 1$. The evolved circle is shown at $t = 10$ and $t = 20$. In the case of the cubic scheme, neighboring points can be seen to diverge very fast. As one might expect, the length of the circle can be numerically verified to increase roughly as the exponent of the maximum Lyapunov exponent. For $\alpha = \beta = 1$ (see Fig. 16), this corresponds to

$$L(t) \sim L(0)e^{0.3t}, \qquad \lambda^{\max} \sim 0.3, \tag{55}$$

where $L(t)$ is the length of the circle at time t. In contrast, large sections of the Nosé-Hoover circle remain smooth at these times indicating regions of stable evolution.

3.9 CORRELATIONS FUNCTIONS

The correlation functions should not be considered independent from the character of the coupling to the heat bath, in contrast to what has been done in the past. The main observation is that ergodicity is determined by the form of non-linear couplings to the heat bath. Different couplings can result in different forms of correlations among the coordinates and momenta in the extended phase space. In Fig. 18, auto-correlations are shown using the cubic coupling scheme (left) and the coupling $F = q$, $G = qp$, $h_1 = \zeta$ and $h_2 = \xi$ (right), both with $\alpha = \beta = T = 1$. In both cases the thermal distributions have been reproduced. As one can see from the figure, the correlations are quite different. Even more significant differences appear between our scheme and the Nosé-Hoover method. Obviously, these facts can be understood qualitatively relatively easily. Both the form and the strength of the coupling to the thermal bath can vary widely from one case to another and the corresponding auto-correlation functions have no reason to be the same. This has to be looked upon as an advantage of the formalism as one can model different physical situations.

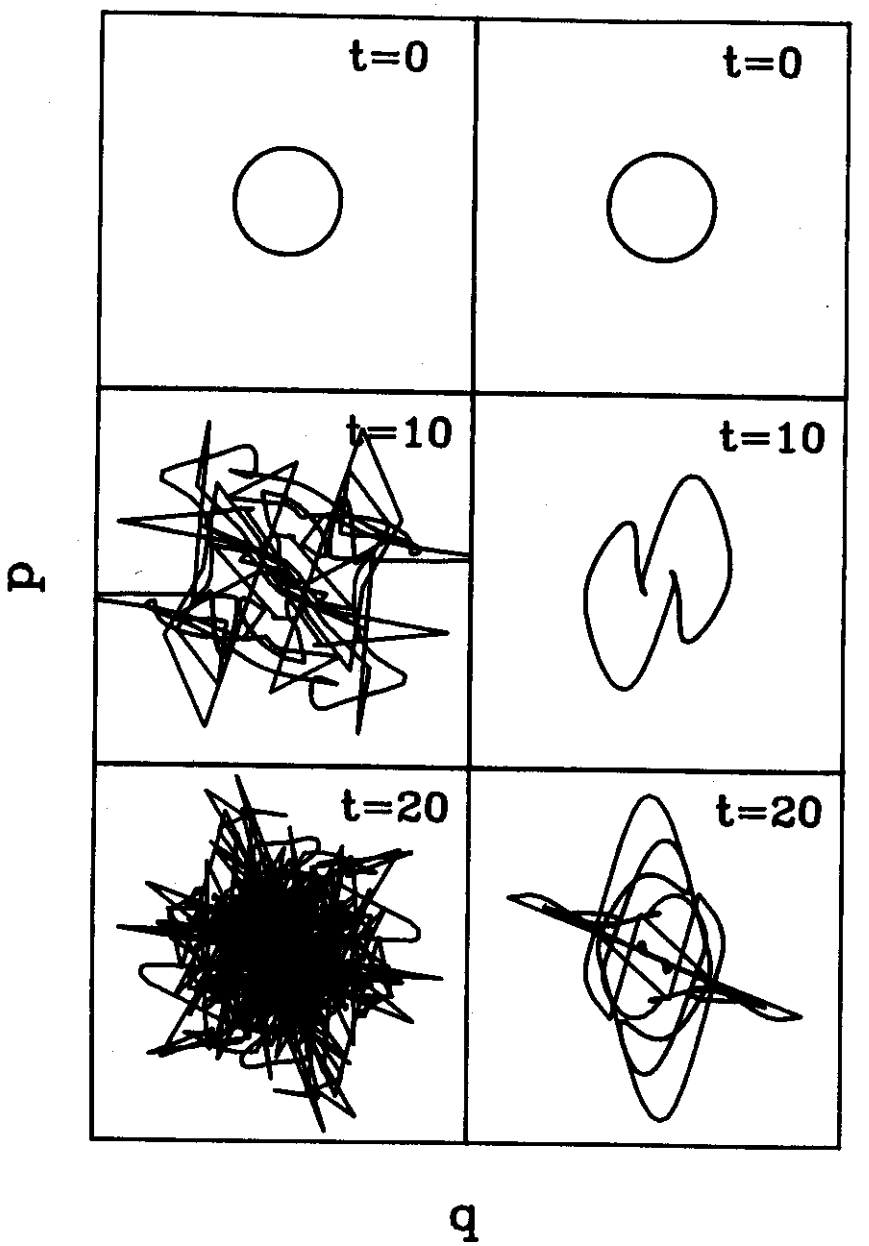

FIGURE 17. Time evolution of a circular initial condition (1000 points) in (a) the cubic scheme with $\alpha = \beta = T = 1$ and in (b) the Nosé-Hoover model with $\alpha = 3, T = 1$ at times $t = 0, 10, 20$. The circle is of radius 1 and the limits are $-3.5 \leq p, q, \zeta, \xi \leq 3.5$.

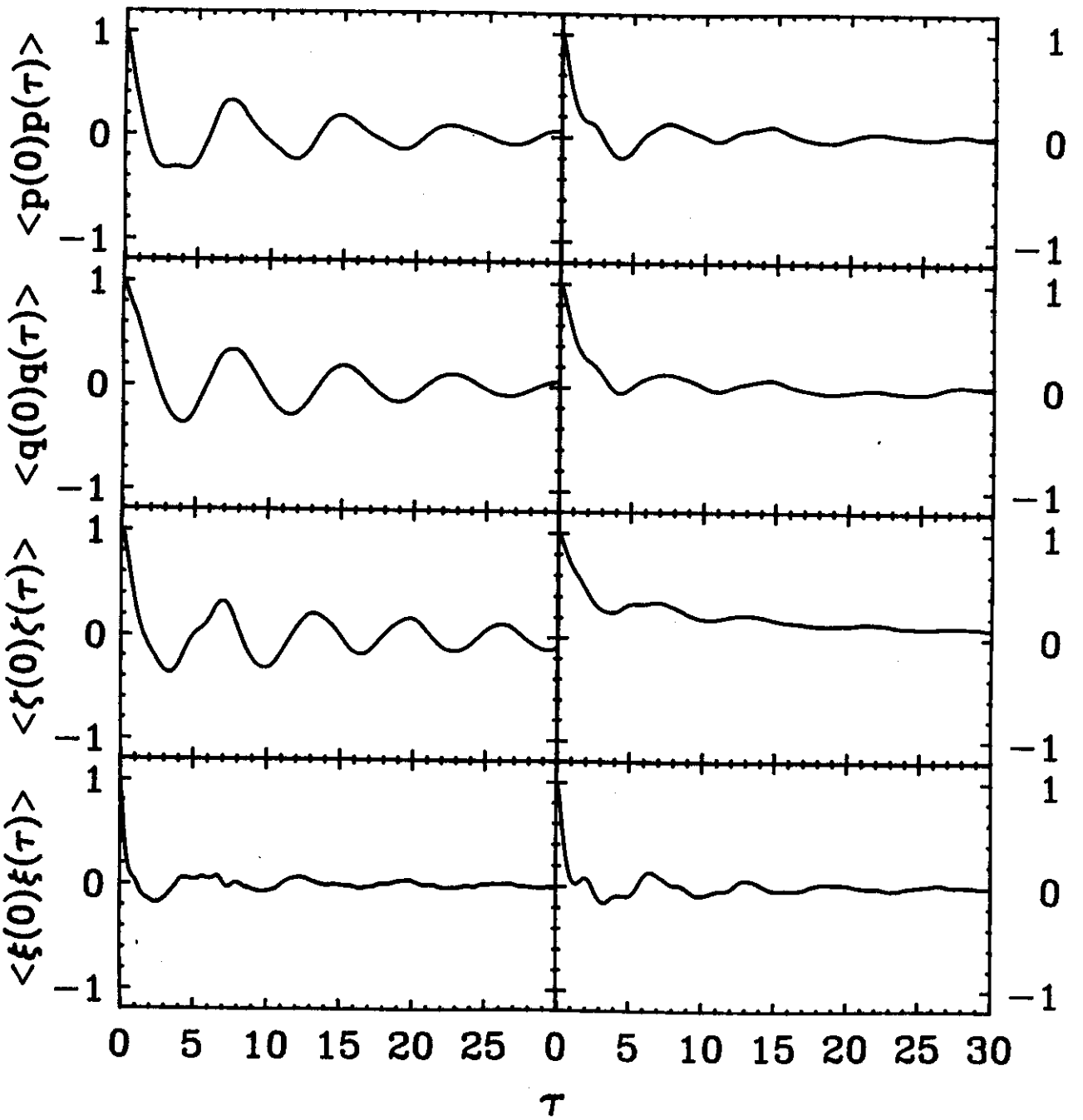

FIGURE 18. Time dependence of auto-correlation functions for a quartic potential in one dimension using the cubic coupling scheme (left) and the scheme $F = q$, $G = qp$, $h_1 = \zeta$ and $h_2 = \xi$ (right) with $\alpha = \beta = T = 1$.

4. CONCLUSIONS

It is obviously very important to have available methods for computing thermal properties for a wide variety of physical systems, which are both reliable and comparatively fast. In almost any area of physics, ranging from molecular dynamics up to lattice gauge theories, different computational schemes have been put forward and extensively used. Among the late newcomers are the methods originating in molecular dynamics calculations, which have found their way into many applications. The method proposed several years ago by Nosé and later on simplified by Hoover was especially successful. This method proved to be easy to implement. However, the studies performed on relatively simple systems pointed to several limitations of such an approach. Especially hard to describe was the case of the harmonic oscillator, which failed to reveal an ergodic behaviour after being coupled to the "thermal bath". The chaotic character of the trajectories generated in this way is an essential element of this approach, since only in this case one can reproduce a thermal distribution by following the trajectory of the envisaged system in time. Also, for relatively small temperatures, when the system is only slightly excited and spends most of the time around the minimum of the potential well, practically every physical system can be approximated rather well with an ensemble of oscillators. Consequently, the correct description of the harmonic oscillator, besides the methodological interest, has a very straightforward practical reason. Moreover, the possibility to produce other types of algorithms was not evident. Besides, the pure theoretical interest, "Are there other types of computational schemes possible?", the more pragmatical question, "Can one produce more efficient algorithms?" was not answered before. On the contrary, it was long believed that such types of approaches are to a certain extent unique.

In the present paper we show how one can easily produce in principle an infinite sequence of similar algorithms. Both the character and complexity of the "coupling" to a thermal bath can be modeled in a wide variety of ways. This situation is obviously very fortunate, since in principle it allows the modeling of any physical situation. We did not try to study or classify all possible computational schemes. We do not know if this is really possible at the moment. We have rather concentrated on a "simpler" generalization of the known methods and "cured" several of their deficiencies, at least those apparent in the analysis of relatively simple systems. We show that the introduction of at least two pseudo-friction coefficients into the Hamiltonian equations of motions is enough to drive the envisaged systems into ergodic motion. This was possible even for the hard to deal with case of the harmonic oscillator. Besides this advantage, the couplings we have studied, proved to be more efficient as well. The rate of their

convergence is higher than that of the methods used previously.

Instead of calculating a few averages, we have compared the generated distributions with the theoretical ones. The agreement we have obtained seems to be limited by the fact that the number of generated phase space points was not infinite but finite. We also showed that chaotic behaviour in the trajectories is not a sufficient condition for the applicability of such methods, since chaoticity does not generally imply ergodicity, which it is what is necessary in such cases. The computational scheme we propose does not only produce a chaotic behaviour, but it possesses at the same time a high degree of mixing. Points in phase space which initially are very close diverge very quickly when evolved using the methods proposed here. In more mathematical terms this can be characterized by larger positive Lyapunov exponents than in previous approaches. The fact that a system has positive Lyapunov exponents does not mean that the system will generally have an ergodic behaviour. From our numerical investigations, it is plausible that the inverse of the maximum Lyapunov exponent has to be of the same order as the characteristic intrinsic time of the system in order to have an ergodic behaviour.

Even though we restricted our presentation to a relatively small sample of examples, we have studied a relatively large variety of situations. It is possible to introduce more than one or two pseudo-frictions coefficients into the equations of motion and in this way to mock the coupling with a thermal bath, which theoretically is characterized by an infinite number of degrees of freedom. This approach generates a simple numerical algorithm, which can be implemented easily and is at the same time stable and numerically efficient.

It is interesting to note that the Hamiltonian structure of the equations of motion is destroyed and in the extended system the symplectic structure of the phase space is lost. It seems that this is a general feature of this type of approaches, which we found necessary to implement in other situations [6,7] , e.g. when the phase space is compact and previous approaches are inapplicable. In such a case the phase space volume is not conserved anymore. However, the Hamiltonian structure of the equations of motion is preserved on average. The additional terms appearing in the extended equations of motion average to zero and the phase space volume is conserved on average.

Support for this research was provided by the National Science Foundation under Grant Nos. 87-14432, 89-06670 and 89-06116.

REFERENCES

1. See for example the review by D.J.Evans and W.G.Hoover, Ann. Rev. Fluid Mech. **18** (1986) 243.
2. H.C.Andersen, J.Chem.Phys. **72** (1980) 2384.
3. W.G.Hoover, A.Ladd and B.Moran, Phys.Rev.Lett. **48** (1982) 1818.
4. S.Nosé, J.Chem.Phys. **81**, (1984) 511; Mol.Phys. **52**, (1984) 255.
5. W.G.Hoover, Phys.Rev. **A 31**, 1695 (1985); "Molecular Dynamics", Lecture Notes in Physics V.258, Springer-Verlag, New York, (1986); H.A.Posch, W.G.Hoover and F.J.Veseley, Phys. Rev. **A 33**, (1986) 4253.
6. A.Bulgac and D.Kusnezov, Michigan State University report MSUCL-696, submitted for pulication.
7. D.Kusnezov and A.Bulgac, in preparation.
8. V.Arnol'd and A.Avez, "Ergodic Problems of Classical Mechanics", Addison - Wesley, Menlo Park, 1968
9. H.G.Schuster, "Deterministic Chaos: An Introduction", pp.114-115 , VCH Publishers, FRG, 1988.